

SPATIAL AND TEMPORAL TRACKING OF PATHOGENIC BIOAEROSOLS IN  
BEEF SLAUGHTER FACILITIES USING DYNAMIC MONITORING  
TECHNIQUES

A Thesis

by

SAMUEL HOWARD BECK

Submitted to the Office of Graduate and Professional Studies of  
Texas A&M University  
in partial fulfillment of the requirements for the degree of

MASTER OF SCIENCE

Chair of Committee,	Yassin Hassan
Co-Chair of Committee,	Maria King
Committee Members,	Alejandro Castillo
	John Haglund
Head of Department,	Andreas Polycarpou

May 2017

Major Subject: Mechanical Engineering

Copyright 2017 Samuel Howard Beck

## ABSTRACT

*Salmonella* and Shiga toxin producing *E. coli* (STEC) have been recognized as pathogens of concern in meats due to the prevalence of this microorganism in the gastrointestinal tract and hide of livestock. Bacterial ingestion due to contaminated food products causes a great economic burden from the hospitalization and death of those who become infected. STEC and *Salmonella* annually cause an estimated 470 deaths in the United States alone. An estimated max of 77.1 billion dollars are lost each year as a direct result of contaminated food. During the harvesting process, these pathogens may become aerosolized from carcass by various mechanisms, including worker activity and airflow from heating, ventilation, and cooling (HVAC) systems.

In this study, one small rural facility and one medium-sized beef facility were examined. High air volume wetted wall cyclone (WWC) bioaerosol samplers capable of concentrating bioaerosols in a liquid effluent were used throughout processing at bleeding, de-limbing, de-hiding, washing, and other stages. Bioaerosols were analyzed using plating and qPCR techniques. Total bacteria count (TBC), STEC concentrations, and *Salmonella* concentrations were enumerated in the air, and critical areas were identified. *Salmonella* and STEC were found to increase with each passing day in the facility, and TBC and STEC increased between morning and afternoon phases of processing. Significant differences in TBC and temperature were found at different locations in the facilities. A novel unmanned aerial system (UAS) capable of capturing bioaerosols at high altitudes was testing

alongside the WWC in cattle feedlots. The UAS performed well, capturing significant concentrations of STEC and TBC.

As of now, HVAC systems have not been studied in correlation with the movement and concentration of bioaerosols in slaughter facilities. Blueprints were obtained from the examined facilities, the cattle processing floors were modeled, and computational fluid dynamics (CFD) were performed. The airflow created from the HVAC systems was found to have an enormous effect on the spread of bioaerosols. Similarities were found between the collected concentrations of bioaerosols and particle traces in the modeled facilities. Finally, new HVAC models were generated for the facilities to significantly increase the sanitation of the beef slaughtering process.

## DEDICATION

To my wife



## ACKNOWLEDGEMENTS

The author would like to extend his sincerest gratitude to his advisor, Dr. Maria King, for her continued guidance and unparalleled support throughout the entirety of his time at Texas A&M University. He also wants to thank Mitch Allain, Mark Garber, Vincent Lau, Darren and Dickens Law, Max Ly, Jeff Shive, Don Vu, and other fellow graduate students for their comradery and assistance. Special thanks is expressed to Gregory and Pamela Beck, the author's parents; without their support none of this would be possible. Thanks to David and Jean Loeb for their loving encouragement. Great appreciation and love is expressed to Carly, the author's wife, for her undying patience and ceaseless care. Finally, thanks to God for whom all things are possible.

## CONTRIBUTORS AND FUNDING SOURCES

### **Contributors**

This work was supervised by a thesis committee consisting of Dr. Maria King, TEES Research Professor, and Dr. Haglund of the Department of Mechanical Engineering, Dr. Hassan the Department Head of Nuclear Engineering, and Associate Professor Dr. Castillo of the Department of Animal Science. The plating analysis carried out in Chapter 3 was performed by Zahra Mohammad. The qPCR data analyzed for Chapter 3 was provided by Dr. King. Dr. King and Zahra both aided in the collection of bioaerosols discussed in Chapter 3. All other work conducted for the thesis was completed by the student independently.

### **Funding Sources**

This work was made possible in part by the North American Meat Institute (NAMI). Its contents are solely the responsibility of the authors and do not necessarily represent the official views of NAMI.

## TABLE OF CONTENTS

	Page
ABSTRACT.....	ii
DEDICATION.....	iv
ACKNOWLEDGEMENTS.....	v
CONTRIBUTORS AND FUNDING SOURCES.....	vi
TABLE OF CONTENTS.....	vii
LIST OF FIGURES.....	ix
LIST OF TABLES.....	xii
CHAPTER I INTRODUCTION.....	1
CHAPTER II REVIEW OF LITERATURE.....	5
II.1 Aerosols.....	5
II.2 Bioaerosol Collection Methods.....	8
II.2.1 Impaction.....	9
II.2.2 Electrostatic Precipitators.....	10
II.2.3 Settling.....	11
II.2.4 Cyclones.....	12
II.2.5 Filtration.....	13
II.2.6 Impingement.....	13
II.3 Heating, Ventilation, and Air Conditioning.....	14
II.4 Computational Fluid Dynamics.....	16
II.5 Process for Slaughtering Beef.....	17
II.5.1 Stunning.....	17
II.5.2 Bleeding or Exsanguination.....	18
II.5.3 Skinning.....	18
II.5.4 Evisceration.....	18
II.5.5 Splitting, Washing, and Chilling.....	19
II.6 Bioaerosols in Beef Facilities.....	19
II.7 Slaughterhouse Associated Pathogenic Bacteria.....	22

II.8 Analysis of Bioaerosols .....	25
CHAPTER III MATERIALS AND METHODS .....	28
III.1 Overview .....	28
III.2 Facility A .....	30
III.3 Facility B .....	32
III.4 Bioaerosol Collectors .....	34
III.4.1 Wetted Wall Cyclone .....	34
III.4.2 Unmanned Aircraft System Collector .....	36
III.5 Preliminary Test .....	37
III.6 Bioaerosol Analysis .....	37
III.6.1 Plating .....	38
III.6.2 DNA Extraction .....	39
III.6.3 qPCR .....	40
III.7 Computational Fluid Dynamics .....	42
III.7.1 Facility A .....	43
III.7.2 Facility B .....	44
CHAPTER IV RESULTS AND DISCUSSION .....	46
IV.1 Facility A qPCR Analysis .....	46
IV.2 Facility A CFD Analysis .....	59
IV.2.1 Original Design .....	59
IV.2.2 New Design .....	67
IV.3 Facility B qPCR Analysis .....	76
IV.4 Facility B CFD Analysis .....	78
IV.4.1 Original Design .....	78
IV.4.2 New Design .....	83
CHAPTER V CONCLUSIONS .....	89
REFERENCES .....	94

## LIST OF FIGURES

	Page
Figure 1: Floor plan of Facility A including all the WWC collector site locations.....	29
Figure 2: Floor plan of Facility B including all the WWC collector site locations.....	30
Figure 3: Front of Facility A.....	31
Figure 4: Middle of Facility A.....	32
Figure 5: Rear of Facility A.....	33
Figure 6: Views inside Facility B.....	34
Figure 7: Open faced WWC's with a 1250 l/min unit on the left and a 100 l/min unit on the right.....	35
Figure 8: UAS collector, with intake doors open.....	37
Figure 9: TBC, STEC, and Salmonella collected each day.....	47
Figure 10: Workers and WWC distance compared to TBC.....	49
Figure 11: TBC, Salmonella, and STEC collected in the morning and afternoon.....	51
Figure 12: TBC, STEC, and Salmonella collected at each site.....	54
Figure 13: TBC compared to temperature and humidity.....	56
Figure 14: Temperature and humidity compared inside the facility.....	58
Figure 15: TBC and STEC collected in feedlot belonging to Facility A.....	59
Figure 16: Skyview of the flow trajectory in Facility A created by dual intakes emitting air at 102.33 ft <sup>3</sup> /s.....	61
Figure 17: Side view of flow trajectories from the dual intakes in Facility A.....	61
Figure 18: The isolated flow trajectory of the intake closer to the front of the facility.....	62
Figure 19: The LMA at head level in Facility A.....	62

Figure 20: Temperature distribution of air inside of Facility A.....	63
Figure 21: Velocity magnitudes at each collector location plotted with the log TBC. ....	64
Figure 22: Skyview of particles released in Facility A.....	66
Figure 23: Skyview of Facility A when 20 particles are released from the entrance of the main hallway to the slaughter floor.....	67
Figure 24: Skyview of the flow trajectories in the new design for Facility A.....	69
Figure 25: Side view of the flow trajectories for the new designs for Facility A. ....	70
Figure 26: Skyview of the LMA near the floor in the new designs for Facility A. ....	71
Figure 27: Skyview of the LMA at head level in the new designs for Facility A. ....	71
Figure 28: Skyview of particles released at the bleeding pit in the new designs of Facility A.....	72
Figure 29: Side view of particles released at the bleeding pit in the new designs of Facility A.....	73
Figure 30: Skyview of particles released from the bleeding pit and de-limbing area in the new designs for Facility A. ....	74
Figure 31: Skyview of particles released from the bleeding pit, de-limbing, and de-hiding area in the new designs for Facility A .....	75
Figure 32: Skyview of particles released at the entrance of the new designs for Facility A.....	76
Figure 33: TBC and STEC collected at each location in Facility B .....	78
Figure 34: Isometric view of the flow trajectory inside of Facility B from the singular fan in the room. ....	79
Figure 35: Side view of the flow trajectory inside of Facility B from the singular fan in the room. ....	80
Figure 36: Skyview of the flow trajectory inside of Facility B from the singular fan in the room. ....	80
Figure 37: LMA and temperature in Facility B. ....	81

Figure 38: Velocity point profiles in Facility B.....82

Figure 39: Particle trace of one hundred particles released from the carcass in the  
bleeding pit.....83

Figure 40: The flow trajectory in isometric view of the new displacement  
ventilation system for Facility B. ....84

Figure 41: Front view of the new HVAC design for facility B. ....85

Figure 42: Isometric view of the flow trajectory coming from the open door. ....85

Figure 43: View of the rear of the facility looking where the freezer door is  
located. ....86

Figure 44: LMA in the new design of Facility B.....86

Figure 45: Isometric views of particle traces in the new design of Facility B.....87

Figure 46: Front view of particles traces in the new design for Facility B. ....88

## LIST OF TABLES

Page

Table 1: Sequence of specific and 16S rRNA oligonucleotides used in the study.....	41
--	----



# CHAPTER I

## INTRODUCTION

Bacteria are the most durable living creatures on earth. They can live in extreme environments and adapt rapidly to altering surroundings. Numerous bacteria, in certain concentrations, pose a serious hazard to humans. Human bodies have adapted well externally and internally to keep out harmful bacteria, including; a dry skin that does not allow bacteria to proliferate, hair and mucus to trap bacterial entry during breathing, and a strong internal immune system. However, one method of entry can easily lead to immediate infection if the internal immune system is overloaded; ingestion.

Bacteria have posed a serious problem to the commercial and private food industries for centuries. Only recently have aerosolized bacteria been seen as a large threat to human health and shelf life of food. The beef industry has a particular hard problem in maintaining a clean environment in the slaughterhouses that process the cattle. The main bacteria that threaten human health with regards to beef are *Salmonella*, STEC *E. coli*, *Campylobacter jejuni*, *Listeria monocytogenes*, and *Staphylococcus aureus* [1]. In particular importance to this study is *Salmonella* and STEC *E. coli*, due to their prevalence and severe pathogenic qualities. *Salmonella* is associated to multiple types of diseases including food poisoning, gastroenteritis, and typhoid fever. *Salmonella* is a gram-negative, rod shaped bacterium that belongs to the family of *Enterobacteriaceae* [2]. *E. coli* belongs to the same family as *Salmonella*, and yet has many differences. The

O157:H7 serotype produces deadly Shiga-Toxins (STEC) that causes 5-10% of people infected to acquire hemolytic uremic syndrome (HUS) [3].

Bacterial ingestion due to contaminated food products causes a great economic burden from the hospitalization and death of those who become infected. STEC and *Salmonella* annually cause 470 deaths. Robert Scharff estimated a max of 77.1 billion dollars lost each year as a direct cause from contaminated food, with STEC and *Salmonella* causing 635 and 12,012 million dollars annually, respectively [4]. However, these costs only take into account the expenses paid by the hospital and the patient. The actual economic burden would be much higher due to the recalls that every establishment has to go through when pathogenic bacteria are found to be in their product.

Although bacteria are robust creatures, many small and easily manipulative environmental changes can disrupt their proliferation. Temperature, humidity, and surfaces play a significant role on bacteria multiplication. Heating, ventilation, and air conditioning (HVAC) systems not only provide necessary moisture for bacterial life, but are also utilized as a means of transport for these microscopic organisms. The direction of airflow can become very important to the sanitation of a facility. Other means of bacterial transport come through worker movement, high pressure washing, running a faucet, drains, and equipment use. The amount of workers, their length of travel in the workspace, and their health will affect the bacteria population. High pressure washing and faucets lift bacteria off the ground and aerosolizes them. Moving equipment also aides in the travel of bacteria. Drains naturally harbor moisture and nutrients for bacteria while over flooded drains will cause the bacteria to become more easily aerosolized. The

majority of harmful bacteria are initially introduced by the cattle. Depending where the cow was before entry into the facility as well as the time of year will affect the amount of bacteria it introduces.

The layout of a slaughterhouse facility will directly affect whether its end products are more likely to become contaminated or not. Walls and dividers between “unclean” and “clean” areas will reduce the likelihood of bacteria traveling from the initial introduction of the cattle to the final stage at the freezer. HVAC systems can inhibit spreading of aerosolized bacteria by utilizing a “down flow” gradient towards the introduction of cattle, as well as placing filters in the ducts to inhibit re-entry of bacteria. If filters are neglected and not changed every few months, bacterial build up will occur. Equipment location and type will also determine if and where bacteria become aerosolized.

Many methods have been developed to enable efficient collection of bacteria. The unique physics inherent to microscopic particles lays direct influence to the different types of collection. The most important characteristics are particle size, number, shape of particles, mass, and composition. Different types of aerosol collectors include impaction, centrifugal, impingement, gravity assist, filters, and electrostatic.

The flow of air around the facility is important for the spread of bioaerosols. The location of ventilation and walls will cause the fluid to spread differently throughout the facility. Also, the location of equipment with respect to airflow could be important for the spreading of bacteria. Depending on the airflow speed throughout the facility, bioaerosols may either settle to the ground, impact on a surface, or follow the flow of air throughout the facility. Therefore, it was deemed important to model the facilities from official

blueprints and utilize computational fluid dynamics (CFD) to visualize the flow patterns in conjunction with experimental results.

The overall project goals were to determine the presence and concentration of Shiga-toxin producing *Escherichia coli* (STEC) and *Salmonella* aerosols in large air volume samples collected at abattoirs using a dynamic air monitoring sampling system. Further objectives included evaluation of reliability for a non-enrichment qPCR method for detecting low levels of STEC and *Salmonella* in the air of beef slaughter establishments and consequential verification of specific identifications by microbial plating on specific media. The HVAC air flow patterns would be modeled from the visited facilities to see the extent of the effect on the spread of bioaerosols, and realize if there was any correlation between HVAC patterns and collected concentrations of bioaerosols. New HVAC models would then be created for each visited facility to increase sanitation of the final meat product. Finally, a novel UAS bioaerosol sampler was tested to collect bioaerosols in feedlots belonging to the abattoirs.

## CHAPTER II

### REVIEW OF LITERATURE

#### II.1 Aerosols

Aerosols are small particles or liquid in a gaseous medium, that the human eye rarely sees, yet they have a large impact on our environment. Sometimes enough aerosols will be in a high enough concentration that humans can see their presence, such as clouds, smog, fog, dust, smoke, and spray paint, for example. Everyday people are affected by the aerosols around them without realizing it. Climate change, the color of sunsets, the spread of disease, pollution, and daily weather are all environmental results of aerosols [5].

From nano-sizes to around 100  $\mu\text{m}$ , aerosols encompass a large range that have different effects on the atmosphere and the human body. By and far the most important aspect of an aerosol is its diameter, commonly referred to simply as particle size. Particles tend to be categorized purely by their diameter. A particles settling velocity may be found by equating the drag force,  $F_d$ , to the gravitational force,  $F_g$ , from Stokes' Law [6]. Large particles experiencing low Reynold's numbers, pulled by gravitational force  $g$ , with diameter  $d$  and density  $\rho$ , will not remain suspended in the air, with dynamic viscosity  $\eta$ , for long and will deposit onto surfaces easily, characterized by the terminal settling velocity,  $V$ , following from Stokes' Law. As well, a large particle has a greater inertia and will exit an airflow more easily than a small particle. Small particles will be carried easily

by any type of flow around a building and can travel great distances on the wind. A small particle may also stay in the air of a room for weeks, even if the air is stagnant.

$$F_g = mg = F_d = 3\pi\eta Vd$$

Solving for velocity:

$$V = \frac{d^2 g \rho}{18\eta}$$

However, the derivation from Stokes' Law is not always correct. For particles that have a diameter,  $d$ , less than 1  $\mu\text{m}$ , a Slip Correction Factor,  $C_c$ , must be used. This is because the particle is now small enough to pass by some gas molecules without being struck, therefore reducing the total force of drag the particle experiences. The mean free path is defined by  $\lambda$ , the average distance that gaseous particles travel between collisions with other gaseous particles [7].

$$C_c = 1 + \frac{\lambda}{d} \left[ 2.34 + 1.05 e^{\left(-0.39 \frac{d}{\lambda}\right)} \right]$$

Now the settling velocity is modified and multiplied by the newly defined  $C_c$ . A particle with a diameter of 15  $\mu\text{m}$  will have a  $C_c$  of 1.01, causing the velocity to increase by 1%. However, a particle with a diameter of 1  $\mu\text{m}$  will have a 15% increase of settling velocity.

Particulate matter under the range of 10  $\mu\text{m}$ , referred to as PM 10, are considered dangerous for human health, and may settle in the bronchioles or alveoli. Fine particles, PM 2.5, are small and light enough to travel very well with the flow of air when humans breath. The particle travels into the pulmonary lungs, and may deposit where gas exchange occurs, in the alveolus. Particles are considered ultrafine when they are less than

0.1  $\mu\text{m}$ . These ultrafine particles are capable of being absorbed into the human body and are especially dangerous [8].

Bioaerosols have all of the traits of their aerosol cousins, but they happen to be from a biological origin. Only recently have bioaerosols begun to be researched, relative to other fields of study. David Sands first studied atmospheric bioaerosols in clouds in 1978 by riding in the passenger side of a prop plane and sticking a petri plate out of one window, later finding *Pseudomonas syringae* where ice crystals had formed [9]. Capable of causing sickness or death at the right concentration, bioaerosols include viruses, bacteria, pollen, fungi, proteins, and spores. The diameter of bacteria are generally within the range of sub-micron to 10  $\mu\text{m}$ , while fungal spores and pollen range from 1  $\mu\text{m}$  to 100  $\mu\text{m}$ . Aerosolization occurs with wind, high pressure spray, worker movement, HVAC systems, coughing and sneezing, and during manufacturing processes. Many bacteria will become dormant while they are aerosolized until they land and reach more favorable conditions. An important characteristic of bioaerosols are whether they are viable or non-viable. Viable bioaerosols have the ability to multiply and increase their concentration. Also, viable bioaerosols can be pathogenic. Unfortunately, humans can create circumstances which favor bioaerosol proliferation and cause concentrations that can be harmful. Factors that affect microbial growth include water, temperature, pH, nutrients, and oxygen. The dark and humid ducts that are used for HVAC systems are great for harboring bacteria, aerosolizing them, and spreading them around. Drains in beef slaughterhouses have water and unwanted bits of fat, creating a perfect environment for bacteria that become aerosolized when sprayed with high pressure hoses or flooding of drains. Steam generated

from clean hot water sinks and hoses in beef facilities creates a warm humid environment for bacteria. Viable bacteria are important for collection if plating is wanted to be done. Aerosolized bacteria are already in a stressed state, and care must be taken during collection. Small aerosols may undergo coagulation from Brownian motion and become a larger aggregate. High flow in an impaction collector can cause cell walls to be destroyed and a dry environment for too long will kill any viable bacteria. However, living bacteria are not needed for DNA analysis.

## **II.2 Bioaerosol Collection Methods**

Many types of bioaerosol collectors have been created and each have their own unique benefits. Before a collection method is chosen, the diameter of the particles of interest should be known. The environment of collection should be analyzed, whether it will be relatively wet or dry. If a collector is to be used outside it must be robust and it should be considered if the collector can be used in the rain. Another concern is how large a sample size needs to be. In many cases, a large volume of air is needed to represent accurately the concentration of bioaerosols. The medium that bioaerosols are transported to are very important as well. Bacteria become stressed during collection, and if the collection period is long or the bacteria are not in a pleasant environment, they will die and not accurately represent their population in the air. Depending on the project, the bacteria may need to be living upon collection. It is wise to plate bacteria to see how many viable colonies have been collected and to sequence the DNA to see how many total bacteria were collected. Most bioaerosol collectors are not capable of collecting a high volume of air, with a long sampling time, high efficiency collection, and viable bacteria. It must be assessed if many



samples are needed, and how close to one another the samples need to be taken. Then it can be decided how complicated of a collector can be used. Some high efficiency collectors take a lot of time to operate, while other methods, such as the sedimentation method, are very simply and can be done quickly. Bioaerosol collectors usually need to be cleaned between samples. If any extent of pipe or tubing is used, it is likely biofilms may form on their surfaces without proper cleaning. This could cause data from collection to be erroneous.

### *II.2.1 Impaction*

One of the most common forms of bioaerosol collection is impaction. Large volumes of air can be pulled through impactors in a short time. Impactors use a pressure gradient to pull in air. The air is usually pulled through small tubes to increase the velocity. When the air reaches the impaction plate the bioaerosols are carried forward by their inertia and adhere to the plate while the air continues on its way around the plate. The length of the inlet tubes that air is drawn through, the distance of the impaction plate from the inlet tubes, the diameter of the inlet tubes, and the velocity of air being pulled through are all very important characteristics for impactors. If the air velocity is too quick, the bioaerosols will die upon impaction, however, if the air velocity is too slow, the bioaerosols will follow the flow of air and never impact on the plate. The inlet tubes should be designed in such a manner that the flow through them is laminar. A turbulent flow will cause a smaller collection efficiency. The impaction plate can be made of various types of media, depending on what type of bioaerosol is wanting to be collected. Certain impact media are used to keep the bacteria viable during and after collection,

others are meant to inhibit any further growth of bacteria, and still others are meant to be selective for one or few bacteria. It should be noted that the large volumes of air that an impactor can pull through may dry out the impaction media quickly. The pressure gradient that causes the suction of air through the impactor is usually created by a vacuum pump, but a fan may be used as well. Impactors can be designed in such a way that they only collect particles under a certain size. These are selective impactors. The Anderson multi-stage impactor is one of the most common. Each subsequent stage has smaller and smaller inlet tubes, causing larger particles to impact on the first plates while smaller particles travel around them and impact later on the last few plates. One of the most important aspects of designing a selective impactor is the diameter at which 50% of particles are collected, or the  $D_{50}$ . If an impactor is said to have a  $D_{50}$  of 2  $\mu\text{m}$ , then 50% of particles with a diameter of 2  $\mu\text{m}$  will be collected. Any particles larger than 2  $\mu\text{m}$  will be collected at an increasing efficiency.

### *II.2.2 Electrostatic Precipitators*

This method utilizes electrical forces instead of inertial forces. Air is drawn across a high voltage field in which bioaerosols experience attraction towards the positively charged end. This is based on a study that most bioaerosols are negatively charged [10]. However, it has been shown that airborne particles can carry both positive and negative charges [11]. This will cause a loss in efficiency and total bioaerosol concentrations will not be accurately known. Some electrostatic precipitators place a petri plate directly over the positive charge, depositing bioaerosols onto the petri plate for impaction and growth. This method does not allow the collected samples to be tested using qPCR or DNA

sequencing. Petri plates that are left open to the air for long periods of time are prone to drying and will cause desiccation, therefore these samplers may not be run for long periods of time. However, the required power to run such devices are generally low, and with no moving parts, they are quite robust and easy to use. Other types of electrostatic precipitators use positively charged corona discharges to make the airborne particles passing through carry a positive charge [12]. A negative rod is then used to collect the newly positively charged aerosols. More recent electrostatic precipitators have become more complex and impact the bioaerosols onto a superhydrophobic half-pipe. This half-pipe is angled at a low incline. While the precipitator is running, small water droplets are intermittently dropped onto the angled half-pipe and the drop collects impacted bacteria and transports them to a vial. This more recent method allows a high concentration of bacteria collection and can then either be used for plating, qPCR, or sequencing techniques. However, the flow rate for these devices is not as high as impactors. Also, bacteria can be harmed by the creation of toxic ozone and NO<sub>x</sub>.

### *II.2.3 Settling*

Gravitational settling is the simplest of all the collection methods. All a user needs to do is place a petri plate in the location of desired collection and open the plate when collection is wanted to begin. This method has the benefits of needing absolutely no equipment operation, saving time, saving cost, the ability to have many petri plates open at the same time, and remaining sterile until collection. However, this collection method is the least representative of bioaerosol concentration. Settling depends on bioaerosols naturally falling onto the plate. If any type of airflow is present in the area of collection,

many small bioaerosols will not actually settle. Also, with no suction, the total volume of air collected is small and incalculable. Settling techniques were used in the past but are largely not used today.

#### *II.2.4 Cyclones*

Cyclones, like impactors, work by using the inertia from airborne particles. The suction is typically driven by a vacuum. Particles enter a cyclone area where the circular motion of air causes the particles inertia to carry the particles to the side of the cyclone walls. Then the cyclones utilize some type of extractor to separate the bioaerosols from the air. Cyclones are capable of even higher flow rates than impactors because the centrifugal motion is more gentle on bacteria due to bacteria impacting at an low angle instead of a head on 90° impact. One problem with many cyclones is that it is hard to get enough centrifugal force to collect very small particles, and particle size cannot be selected for. Some cyclone collectors use a liquid to help ensnare entering bioaerosols. A liquid will be aerosolized and injected into the oncoming stream of air. Bioaerosols either become ensnared in the droplets, or become collected upon impact in the cyclone. Then, down-flow of the entrance, the spinning fluid is skimmed off the surface of the cyclone, while the air exits through the exhaust. The skimmed liquid with bacteria is pumped into a sterile collection tube. This method allows for high volumes of air to be collected as well as for a high concentration of bacteria. Cyclones tend to cost more than other methods of collection, but they are compensated with more air volume collected, higher efficiency, the capability to keep the bacteria viable, and a high concentration of bacteria in a liquid ready for many different types of analyses.

### *II.2.5 Filtration*

The filtration method is much like impaction, but instead the airflow is drawn through a fibrous filter. The fibers cause 3 different forms for contact of bioaerosols to filter. Interception happens when a particle following the air stream comes within one particle radius of a fiber and thus attaches to the fiber. Impaction occurs when the particle following the air stream is unable to follow the flow of air and its inertia carries it to impact on the fiber. The third form of contact happens to smaller particles which experience Brownian motion and the particle deposits on the fiber by diffusion. Bioaerosols are more likely to survive attaching to a fiber on a filter than impaction, but a system using a filter usually has significant pressure losses. The mechanical aspects of filters depend mainly on the size of the fibers that make up the filter, the velocity of the air stream, and what size particles are wanted to be collected. The filters have a large surface area that causes the attached bacteria to experience a lot of airflow and subsequently desiccate quickly. Therefore, sampling times need to be short to ensure viability of the bacteria. Filters need to either be stamped onto petri plates or placed into a liquid and agitated to knock the bacteria off the filter. Then qPCR, serial dilutions, or DNA sequencing can be accomplished. When the filter is taken out of the collection device and placed into liquid media, the filter has a chance of becoming.

### *II.2.6 Impingement*

An impinger uses a vacuum to draw air through an inlet and through a small body of liquid. The air is pulled out through the exhaust while bioaerosols impinge into the liquid and become trapped. If the velocity of the oncoming air is too high, bacteria may become

injured. Impingers also have a hard time having a high flow rate because the liquid the particles are impinging on displaces more and more with greater air velocity. However, impingers do have the benefit of depositing the bioaerosols immediately into liquid, allowing an impinger to run for very long periods of time while allowing the bacteria to remain viable. Another problem that may arise with impingers is the bubbles that are formed when the air is drawn through the liquid. Bacteria can be entrapped inside the bubble and be carried out through the exhaust, decreasing efficiency and true knowledge of the concentration of bacteria in the air. However, impingers have been demonstrated to be particularly good at collecting viruses.

### **II.3 Heating, Ventilation, and Air Conditioning**

Heating, ventilation, and air conditioning (HVAC) are used in almost every single building in the United States. Indeed, one of the main expenditures of building and maintaining a structure is the HVAC system. The comfort, safety, and work productivity of humans is dependent on a well working HVAC system. Industrial buildings consume 69% of their total energy expenditure to heating, and 8% to both cooling and ventilation. The food manufacturing industry has the highest amount of non-office floor space and the second highest amount of floor space over all other types of industries. The food industry is also the highest consumer of energy along with transportation equipment among industries [13]. The problem with HVAC systems, in this case focused particularly in slaughterhouse facilities, is the filtration system and direction of airflow. Ventilation has been shown to be effective in eliminating ozone, and even better at eliminating ozone when particles, organic and inorganic, build up the filter [14]. The harm happens when

bacteria latch to the wall of material and form colonies. Filters can be treated with a bactericide that stops the buildup and release of bacteria for 67 days, however, untreated filters release bacteria after 27 days [15]. It is well known that the inadequate cleaning of ventilation will lead to economic losses and the development of disease in employees, visitors, or final consumers [16, 17]. Humidifiers are usually the cause for the proliferation of bacteria. In slaughterhouses where humidity can be very high, bacterial growth can be a much bigger problem than in commercial buildings where the relative humidity is kept much lower. Microbial contaminants, including *Staphylococcus aureus*, were found in all production areas of a burger plant even though the rooms were physically separated by walls [18]. A study by Prendergast et al. showed that the layout of slaughter facilities is important to airborne bacterial concentration. The authors compared two slaughter facilities and found the facility with a straight production line and one level had the lesser amount of contamination [19]. Another study showed that *Salmonella* in the air contaminates meat products even when stored in low temperatures [20]. Temperature and relative humidity variations should be kept to a minimum since both factors have such a large impact on microbial growth and temperatures should be kept below 55.4 °F. At this point no study has been performed to analyze the HVAC systems of beef slaughterhouse facilities using computational fluid dynamics (CFD) in order to find problematic areas within the facilities and relate that to experimentally found concentrations of bacteria in said facilities.

## **II.4 Computational Fluid Dynamics**

Computational fluid dynamics (CFD) has been around for a relatively short time but was pioneered a century ago by Richardson [21] and has revolutionized the way products are designed and manufactured by saving time and costs. Many different CFD software platforms exist and every year each one becomes more powerful. There have been many debates about each of the opposing CFD platforms, and which one is more computationally proficient. The food industry has adopted CFD to aid in refrigeration, mixing, cooling, sterilization, and drying, which corresponds to increased shelf life and food safety. Field experiments used alongside CFD to visualize fluid currents has been used in the past to give insight to different aspects of food production facilities such as contaminant sources and room design [22]. Other studies have committed themselves to calculating the amount of fresh air delivered and contamination removed by tracking airflow in the room, such as the study by Rouaud and Havet, whose experimental results showed contamination of a room is largely dependent on the location of initial contamination, displayed use of contaminant removal effectiveness equations to garner the efficacy of ventilation systems, and used the room mean age of air to determine mean decontamination time [23]. SolidWorks Flow employs the Navier-Stokes equation in conjunction with a finite volume discretization that divides the computational domain into elementary volumes around every node in the grid, ensuring the flow between nodes is continuous. Tetrahedral interpolation is used for spatial discretization, while temporal discretization utilizes the implicit formulation. A study by Driss et al. used SolidWorks Flow to characterize the turbulence around a Savonius wind rotor, and validated their



SolidWorks calculations with experimental results [24]. SolidWorks uses an empirical, modified two equation  $k-\epsilon$  turbulence model along with immersed boundary Cartesian meshing that allows a wide range of turbulence models to be calculated correctly with the utility of low density mesh sizes. In these equations  $K$  is the kinetic energy and  $F$  is the dissipation rate of turbulent energy. The  $k-\epsilon$  model has been used effectively to model room airflow, including forced convection [25]. An alternative to this method is the Large Eddy Simulation (LES) model that has received much attention and is capable of calculating real time turbulent flow, as opposed to the steady state solution found by the  $k-\epsilon$  model.

## **II.5 Process for Slaughtering Beef**

### *II.5.1 Stunning*

According to the Humane Methods of Slaughter Act of 1978, all animals slaughtered in the industrial food process business are required to be stunned before bleeding. First the cattle are rested for a period of time, the recommended amount being 24 hours in a feedlot. The cattle are transported to the processing facility and walked into a stunning box. A stunning hammer or a captive bolt stunner, the most common, is used on cattle between the eyes for immobilization. Depending on the size of the facility the cattle are either hung mechanically by the rear leg right after stunning, or they are dropped on the floor and hung from the rear leg by a worker. Both methods can cause the release of bacteria from the cattle hide.

### *II.5.2 Bleeding or Exsanguination*

The actual death of the animal occurs due to cerebral anoxia when the main blood vessels of the neck are cut. The 30 cm cut is performed with a knife between the jaw and brisket. Then a clean knife is inserted a 45° angle to sever the jugular and carotid vessels. It takes about six to nine minutes to bleed out cattle.

### *II.5.3 Skinning*

Before cattle skinning can be performed, the head and legs must be removed. After the animal has bled out, the head is skinned and severed by cutting through the occipital joint and neck muscles. The head is saved for inspection. The fore and hind legs are also skinned and removed. The anus is cut and loose and tied off. Then the cattle are flayed by cutting a line from the sticking line to the tail. In large facilities, automatic hide pullers are used to pull the skin from either the hind or the rump. The less contact the carcass has with operators, the less chance there will be of bacterial contamination, however the mechanical process of pulling the skin of the animal aerosolizes a very large amount of bacteria.

### *II.5.4 Evisceration*

The carcass, still hanging vertically, is cut down the middle of the abdominal cavity with a saw. The gastrointestinal tract is tied to prevent contamination. A worker cuts around the stomachs, spleen, and intestine. The viscera then fall to the floor from gravity. The viscera are separated into the paunch, intestines, and thoracic viscera for inspection. If any parts are meant for human consumption they are tied off to inhibit cross contamination. The kidneys are left on until the carcass has been split.

### *II.5.5 Splitting, Washing, and Chilling*

A worker faces the back of the carcass and uses a power saw to cut down through the middle of the spine. The saw should be sterilized in 180-190 °F water, one aspect of slaughterhouse facilities that leads to high humidity and variation in temperature. The beef is then carefully trimmed for excess fat and inspected for bruising or fecal contamination. The beef needs to be washed, but it must not be washed for too long or bacterial contamination is more likely to occur. Sometimes an organic acid wash is applied. The carcasses are weighed and then quickly moved into the chiller, keeping the meat dry as possible to inhibit bacterial growth. After 36 hours the deep muscle tissue should be at 42-44 °F. The air inside the chiller has an air speed of around 0.5 m/s to cool the carcasses quicker by forced convection. Relative humidity should not rise of 90%. Warm carcasses moved into a chiller will experience condensation and be more prone to mold and bacteria growth. The chiller should be kept at 30.2 °F, but many industrial facilities fail to meet this criteria and thus the meat will have a shorter shelf life.

### **II.6 Bioaerosols in Beef Facilities**

The presence of microorganisms in the air of meat harvesting establishments, with the consequent transfer of such microorganisms including potential pathogens to the carcasses, is a well-documented fact [26-29]. Some of the major sources of contamination in meat processing facilities are bioaerosols generated from wastewater, rinse water, cattle hides, and spilled product that become aerosolized. HVAC systems contribute airborne microorganisms under normal operation because they provide fertile areas for growth due to moisture and darkness. Worker activity (including talking, sneezing, and coughing),

equipment operation, sink and floor drains, and high pressure spraying are also major sources of bioaerosols [30, 31]. Of greatest concern in the meat industry is the possibility of generating bioaerosols containing bacterial pathogens. *Salmonella* and STEC have been recognized as pathogens in beef due to the prevalence of these microorganisms in the gastrointestinal tract of cattle [32-34]. Airborne transmission of bacterial pathogens such as *Salmonella* and STEC to the surface of cattle and pigs may occur since the farm stages [35]. These pathogens may be transferred to the carcasses during harvesting by bioaerosols formed particularly at specific processing areas such as the hide removal area at beef harvesting establishments, where air and droplets are more likely to be aerosolized [28, 36]. Air sampling at food plants is useful to identify likely sources of airborne contamination with foodborne pathogens and improve plant sanitation programs. Information on populations of total plate counts, lactic acid bacter, yeasts and molds etc. in the air of food and other types of premises have been available since the 1950's and 1960's [37, 38]. However, reports on the prevalence of bacterial pathogens in the air of harvesting plants are not easily available. Studies of airborne pathogens in slaughter plants have reported either absence, low incidences, or low concentrations of pathogens, especially regarding *Salmonella*, *Listeria monocytogenes*, or STEC [27, 28, 36, 39]. However, most of these reports have used a plate sedimentation method for sampling. These methods typically involve the collection of a relatively low volume of air resulting from sampling at a low air flow rate for a time ranging between a few minutes to hours. Sampling for a longer time to collect a larger air sample generally involves sample dehydration, with consequent stress to the bacteria. The low recovery of microorganisms

in air samples collected by traditional bioaerosol sampling methods, such as spore traps, impingers, nucleopore, and gelatin filters has been known for several decades [40, 41]. This limitation is mainly due to biological stress during the sampling process [41], and by the small volume of air sampled and hence the quantification that can be achieved. For example, the Andersen 6-stage viable particle sizing sampler (6-STG), which is one of the samplers of choice for the collection of viable microorganisms and outperformed 7 other air samplers in a controlled study [42], is commonly set at a flow rate of 28 liters per minute and let to sample for 15 minutes. Schmidt et al. [36] placed sampling sponges in specific areas of three slaughterhouse to determine bioaerosol counts by sedimentation with exposure times ranging from 30 to 120 minutes. They theorized that areas with droplet spray, specifically near the hide removal process, caused a higher aerobic and pathogenic bacteria count. No pathogenic bacteria were detected in the fabrication areas, assumptively because the airflow systems at each of the three establishments was design to direct airflow from “clean” areas to “dirty” areas, but as a sedimentation method was used throughout the study, these results are likely not accurate. Cattle hides are a major source for pathogenic aerosols in beef facilities. Testing in cattle feedlots, Chopyk et al. [43] found *E. coli* O157:H7 on cattle hides and in feces, while also discovering a significant correlation between low-diversity bacterial communities and the presence of pathogenic *E. coli*. In a similar study by Beach et al. [32], *Salmonella* tracked from beef feedlots to the knocking pen of slaughterhouses saw an increase in concentration from a max of 20% to 56%. As well, nineteen percent of cattle were tested positive for *Salmonella* and 54% of carcasses were positive for *Salmonella*. Therefore, there is a need to do more

testing inside of beef slaughterhouses and in the feedlots where cattle reside before going to said slaughterhouses to see how the microbial populations are related. At a modern high throughput cattle slaughterhouse, Jericho et al. [26] found that the highest total viable count of bacteria occurred at the hide pulling areas. Sanitation is monitored at the facility using critical control points, however, while the facility had not considered bioaerosols as a critical control points, the authors recommended that it should be so, specifically at the hide removal floor. Rhakio and Korkeala tried to analyze the movement of airflow in beef and pork slaughterhouses with air current tubes, but failed to do so. The HVAC of slaughterhouses needs to be modeled using CFD in conjunction with experimental sampling to get a good perception of the actual airflow of the facilities.

## **II.7 Slaughterhouse Associated Pathogenic Bacteria**

People have known about foodborne diseases for a long time, and while manufacturing processes become larger and quicker to meet the demand of an exponentially growing population, new problematic diseases arise on top of the ones of old. From *Bacillus cereus* poisoning in 1906, to *Salmonella typhimurium* outbreaks in 1953, with *Yersinia enterocolitica* developing in the 70's, and finally *Escherichia coli* OH157, *Campylobacter*, and *Listeria monocytogenes* appearing in the 80's [44, 45]. Pathogenic bacteria are introduced into beef slaughterhouses by the gastrointestinal tract of cattle, the hide of the cattle, and from workers. Once introduced, the slaughterhouse facilities do a good job of maintaining a beneficial environment to promote more bacterial growth [46]. Beef that is refrigerated will still spoil because of bacteria such as *Carnobacterium* spp., *Enterobacteriaceae*, *Pseudomonas* spp., *Leuconostoc* spp., *Lactobacillus* spp., and

*Brochothrix thermosphacta* [47]. The particular troublemakers in beef that cause disease are *Salmonella* spp., *Escherichia coli* O157:H7, *Listeria monocytogenes*, and *Staphylococcus aureus*.

*Enterobacteriaceae* is a very large family of gram-negative bacteria with some living in the intestinal tract of humans and animals. They are facultative anaerobes that do not form spores. Dr. Daniel Salmon was a veterinary pathologist who first found *Salmonella*. *Salmonella* is a rod shaped bacterium with diameters from 0.7-1.5  $\mu\text{m}$  and lengths of 2-5  $\mu\text{m}$ . Capable of causing typhoid fever, foodborne illnesses, and paratyphoid fever, it is not a bacterium to be trifled with. Many of the infections *Salmonella* causes is from people ingesting contaminated food. As of today, there are three known species that include *Salmonella enterica*, *Salmonella bongori*, and *Salmonella subterranean*, with many serotypes. The main habitat of *Salmonella* is in the intestinal tract of humans and animals, and while some species do not cause any bad symptoms in humans, others will cause infections called Salmonellosis. Refrigeration will not destroy *Salmonella*, but rather inhibit the growth of *Salmonella*. The serovars of *Salmonella* that are of the most concern are *Typhi*, *Typhimurium*, and *Enteritidis*. Generally, infection of *S. Typhi* is a result of ingesting infected water and produces symptoms such as fever, vomiting, nausea, and possible death. *Typhimurium*, on the other hand, is usually not fatal, but causes symptoms of cramps, vomiting, nausea, and diarrhea for about a week. Lastly, *S. Enteritidis* causes most of the food poisoning in the United States and has symptoms like *S. Typhimurium*. Upon ingestion, *Salmonella* makes its way into the intestines, and passes through the intestinal wall using special proteins on its surface. Then, it makes its way to the liver or

spleen, where it can grow and release more *Salmonella* into the intestine. *Salmonella enteritidis* will either die out after a week in the human body or else be treated with gentamicin or ampicillin. However, some people develop Reiter's syndrome, known to cause pain in joints, urination, or eyes and can last for years or even cause development of chronic arthritis. In a 2011 study, *Salmonella* was estimated to cause 1,029,382 illnesses, 19,533 hospitalizations, and 378 deaths [48, 49]. *Escherichia coli* belongs to the same family as *Salmonella*, and is thus very similar. *E. coli*, discovered by Theodore Escherich in 1885, is rod-shaped and gram-negative, and under favorable conditions it takes only 20 minutes to reproduce. The size range of *E. coli* ranges from 0.25-1  $\mu\text{m}$  in diameter and 2  $\mu\text{m}$  in length. *E. coli* O157:H7 was discovered as a pathogen in 1982 from fast food restaurant hamburgers after an epidemic of hemorrhagic colitis [50]. One of the most potent toxins, Shiga toxins, are produced by this serotype of *E. coli* [51, 52]. The reason Shiga toxins are so potent is because they inhibit protein synthesis in cells, however, endothelial cells, which line the inside of blood vessels, are more susceptible to this cytotoxigenic toxin [53]. As well, *E. coli* O157:H7 is capable of colonizing bacteria in the intestines and lysing red blood cells while liberating iron to help its own metabolism [54]. The CDC has recognized the pathogen for its large threat to public health. Meat products are not the only cause for outbreaks of O157:H7, other outbreaks have been found in many other types of food products [55, 56]. *E. coli* of all serotypes is estimated to cause 2,429 hospitalizations, 205,781 illnesses, and 20 deaths, with serotype O157:H7 causing 2,138 hospitalizations, 63,153 illness, and 20 deaths [48, 49].



## **II.8 Analysis of Bioaerosols**

Upon collection of bioaerosols, a certain analysis method needs to be chosen. Typically, before collection of bioaerosols begins, the analysis method for post-processing needs to be known. Various kinds of analysis methods exist, and as time has gone on since the study of bioaerosols, the analysis methods become more powerful. As new methods of analyzing microbes arose, a subsequent change in bioaerosol collectors began. Initially, all bioaerosols were examined by plating onto agar plates. Impactors and centrifuges were designed in such a way that the bioaerosols would impact directly onto agar plates, cutting out a step in post-processing by eliminating the need to make spread the sample manually. After collection, the liquid from impingers is spread onto agar plates. After an incubation period, the agar plates are inspected for colony forming units (CFU's) and total viability count (TVC), then divided by the total volume of air sampled. However, this method of analyzing bioaerosols only measure viable bacteria, any bacteria harmed in collection or in too low of a concentration to form colonies, are not taken into account. As well, some bacteria may not grow on agar because the agar is either selective against the bacteria, or other species of bacteria outcompete each other. For this reason, a simple agar is chosen that will help growth of most bacteria such as nutrient agar, casein soy peptone, and tryptic soy agar. Sometimes many different types of culture medium may be needed to asses all types of aerosolized bacteria and many replicate samples need to be taken. However, this remains a problem because the total bacteria count remains unknown [57]. Phenotypic and genotypic characteristics of the bacterium are explored to enumerate its species. In order to identify the type of bacteria after plating, phenotypic techniques

such as gram stains, microscopy morphology, vulnerability to antibiotics, and metabolites are observed. Other types of analyses utilize antigen-antibody reactions such as enzyme-linked immunosorbent assays (ELISA) and immunofluorescent assays. However, genotypic identification utilizes the genome of the collected bacteria, acting as a conclusive result. These molecular methods include the polymerase chain reaction (PCR), real time PCR, electrophoresis, and many more. Many analysis techniques changed with the arrival of PCR. Now it no longer mattered if collected bacteria were viable, all that was needed for analysis was the DNA of the bacteria. With the capability of amplifying the amounts of DNA exponentially in a few hours for inspection, long days of culturing seemed to be obsolete. As well, it is now more optimal to collect bioaerosols into a concentrated liquid instead of directly onto an agar plate, hence changing how collectors were designed. The next large breakthrough after PCR was genomic sequencing techniques. Instead of single amplicons being used to find out total concentrations of a single bacterium, now with genomic sequencing the entire microbiome of a sample can be mapped and the percentage of every bacterium in the sample is known. Illumina DNA sequencing needs the DNA of bacteria to be broken into fragments ranging from 200 to 600 base pairs. The fragments are incubated inside sodium hydroxide with adaptors to form single stranded DNA. The DNA moves across a flow cell where primers will bind to correlating pieces of DNA. Any DNA that has a primer attached is latched in the flow cell and will display a signal that is picked up by a camera. Nucleotide bases and DNA polymerase are then added to form double-stranded DNA, which is then broken into single-stranded DNA, leaving many identical pieces of DNA sequences. Although this

method increased the power of post-processing, it did not shape the way bioaerosol collectors were built. Fluorescent terminators that correspond to different bases (A, C, T, G) are added that, when a laser is passed over, become detected by a camera and recorded on a computer [58]. This new method is accurate, fast, and much cheaper than other DNA analysis techniques. After the DNA has been sequenced, analysis tools such as QIIME can be used to look at the sample and find out what percentages of species, relations occurring in the microbiome of the sample and separate samples, and creating publication ready images of data.

## CHAPTER III

### METHODS AND MATERIALS

#### III.1 Overview

Air samples were collected from inside two different beef slaughtering facilities, A and B, within a three-hour radius of College Station. Dynamic, fifteen-minute air samples were collected during processing hours at the bleeding, de-limbing, de-hiding, and spine splitting/washing stages. As well, long term samples were taken inside each facility that would collect the entire day, placed in important areas of interest, including the de-hiding area and near the chiller entrance. All air samples inside the facilities were collected using Wetted Wall Cyclones (WWC). The continuous WWC units were set to intake air samples at 100 liters/min. The dynamic sampling WWC collected all samples at 100 liters/min. The sampling locations for facility A and B are represented in Figures 1 and 2, respectively. Facility A is a small facility with a possible throughput of 8 cattle per day. Facility B was a small, local facility with a throughput of about 3 cattle per day. Air samples were collected in a feedlot belonging to facility A using a 100 liter/min WWC and novel UAS collector the day before cattle were sent to the slaughter facility. After collection, the samples were plated within the same day. Also, qPCR was performed for all the samples.

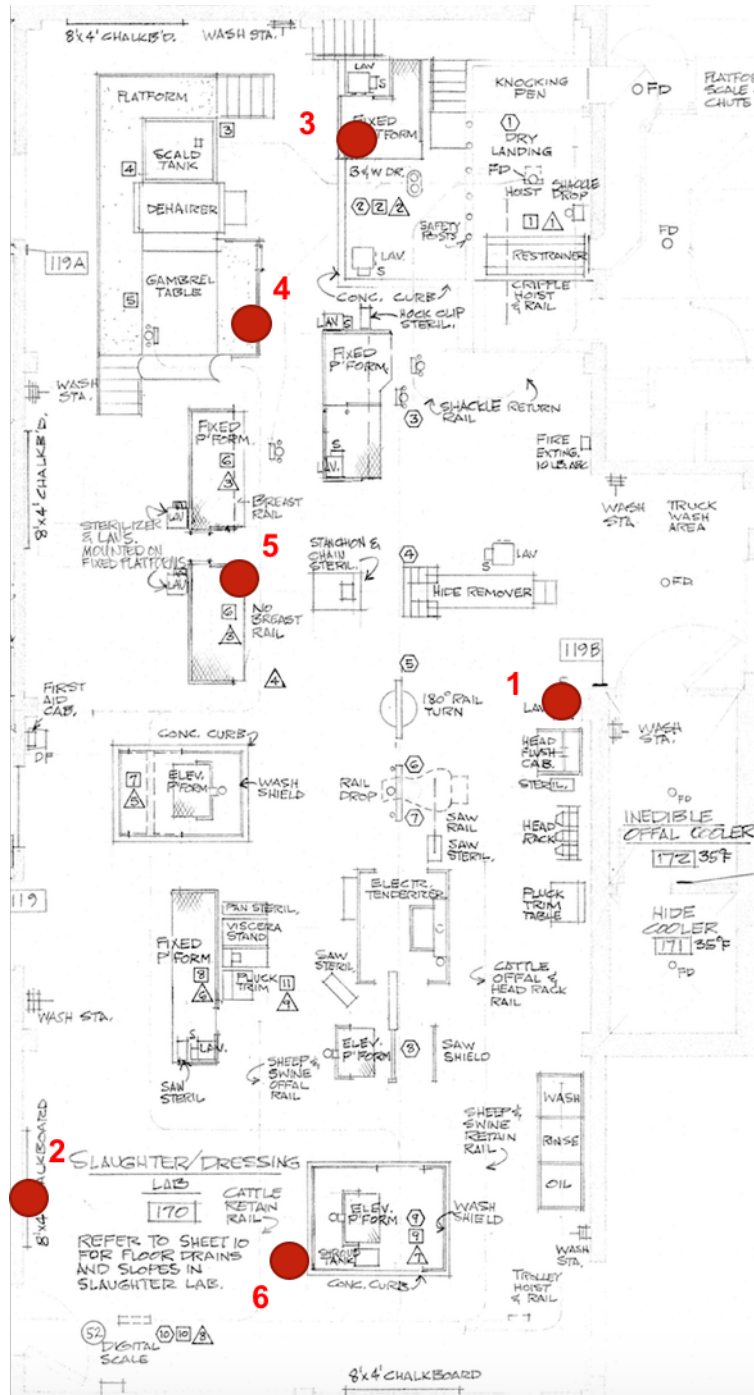


Figure 1: Floor plan of Facility A including all the WWC collector site locations. 1-Continuous WWC near de-hiding. 2- Continuous WWC near freezer. 3- Dynamic WWC bleeding pit. 4- Dynamic WWC de-limbing. 5-Dynamic WWC de-hiding. 6- Dynamic WWC splitting/washing.

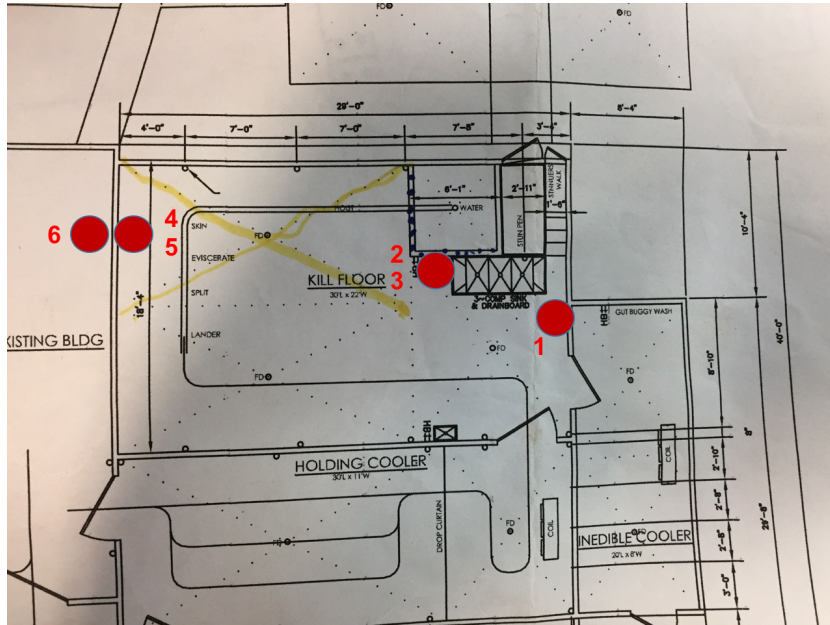


Figure 2: Floor plan of Facility B including all the WWC collector site locations. 1- Continuous WWC near freezer. 2 and 3- Dynamic bleeding and de-limbing. 4 and 5- Dynamic de-hiding and washing. 6- Dynamic outside hallway.

### III.2 Facility A

Bioaerosols were collected at Facility A for three consecutive days from October 25, 2016 to October 27, 2016. The facility consisted of one large rectangular room with no walls separating clean and unclean areas, with processing beginning at the front and continuing in a straight line to the rear (Figures 3-5). Sampling sessions were broken into two phases, including morning phase and afternoon phase. During both phases, four cattle were processed. When processing began, both continuous WWC collectors, operating at 100 l/min were started, one near the de-hider and one at the rear of the facility near the chiller. As well, when the first cattle were introduced, the dynamic sampler was operated at 100 l/min for fifteen minutes at each stage. The stages of sampling ran in sequence from bleeding, de-limbing, de-hiding, and spine splitting/washing. Two Hobo® data logger

units were placed on top of the continuous WWC samplers to measure temperature and relative humidity (RH) during the entire process. They have an accuracy of +/- 0.95 °F and +/- 3.5% RH and were sampled every five seconds. The morning phase was complete when all four cattle had been processed and the same process began again in the afternoon, continuing for a total of three days.



Figure 3: Front of Facility A. (Left) WWC near the bleeding pit. (Right) WWC near the de-limbing area.

On a later date, January 24, 2017, bioaerosols were sampled from the feedlot belonging to Facility A. The cattle inside this feedlot would be processed at the facility the next day. A single WWC unit, running at 100 l/m, was placed downwind of the cattle and set to sample for fifteen minutes. This was repeated three times. The UAS sampler was also brought to the feedlot and sampled a single time for ten minutes alongside the WWC collector. Temperature, RH, and wind direction data were taken from the SparkFun HH 6130 sensor and the rotary encoder onboard the UAS. On the next day, January 25, 2017,

the cattle from the feedlot were processed in Facility A. The same procedures were followed as before, however, all eight cattle were processed in the morning phase, therefore no samples were taken in the afternoon.



Figure 4: Middle of Facility A. (Left) WWC near the de-hider. (Right) View from the rear of the facility.

### III.3 Facility B

Bioaerosols were collected at Facility B for one day on January 31, 2017. This small, local facility consisted of a single room used for slaughtering cattle (Figure 6). All processes, bleeding, de-hiding, eviscerating, and washing all took place in nearly the same location. One continuous WWC, operating at 100 l/min, was placed next to the door of the chiller. The other dynamic sampler, running at 100 l/min, was used to sample at the location of bleeding, de-limbing, de-hiding, and in the hallway outside of the slaughter room. The dynamic collector stayed in the same location for bleeding and de-limbing since



the carcass had not moved. As well, the collection of samples by the de-hiding and washing process were in the same location due to the carcass not moving, reference Figure 2. All samples were collected in the morning. Two Hobo® units were again used to measure temperature and relative humidity. One was placed on top of the continuous WWC collector, and the other was placed near the door leading to the hallway from the slaughter room.

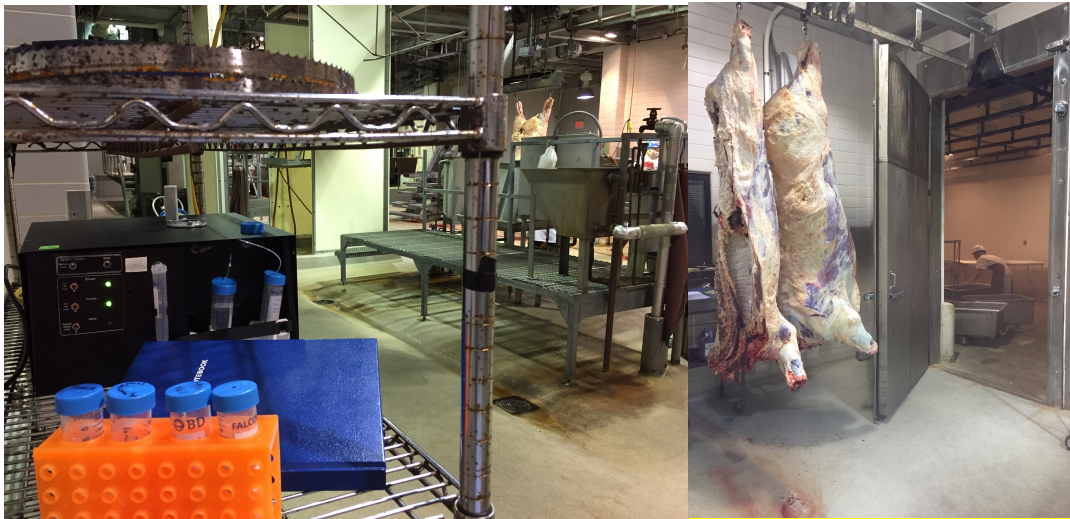


Figure 5: Rear of Facility A. (Left) View from rear of the facility where collector #2 is positioned. (Right) Carcasses entering freezer door.



Figure 6: Views inside Facility B. (Left) Facility B, view of the knocking pen and continuous WWC unit near the freezer door. (Right) View from the freezer door facing the doorway out into the hallway.

### **III.4 Bioaerosol Collectors**

#### *III.4.1 Wetted Wall Cyclone*

The WWC is a cyclone bioaerosol collector designed for high efficiency, large air intake, and concentration of aerosolized bacteria into a hydrosol (Figure 7). The intake speed of a WWC can be set to various volumetric flow rates depending on the project at hand. This adaptable device first aerosolizes liquid to a median size of 40  $\mu\text{m}$  with an atomizer into the entrance cavity, directed into the oncoming flow of air. The liquid input allows a film to be formed onto the cyclone, where the bioaerosols impact onto. A vortex finder inside of the cyclone aides in the creation of uniform vortex flow. As air flows towards the exhaust, the speed creates a shear force that carries liquid towards a skimmer, where the newly formed hydrosol is separated from the exhausting air, leaving a

concentrated bioaerosol solution. The concentrated hydrosol effluent flow rate is 0.1 mL/min which creates a concentration factor of  $0.87 \times 10^6$  for particles in the range of 1.2-8.3  $\mu\text{m}$  and a pressure differential of 6.4 inches water. The WWC cutoff point for aerosol to hydrosol efficiency is 1.2  $\mu\text{m}$  and has a particle collection efficiency of 86% for aerosolized *Bacillus atrophaeus* from 1.2-8.3  $\mu\text{m}$  [59]. When the WWC was compared to a different type of impactor for the viable collection of large *E. coli* DNA strands (500,000 bases) the WWC collected significantly more viable strands [60]. All of the WWC collectors were completely cleaned before each collection day by running 10% bleach through the collectors, followed by isopropanol, and finished with Milli-Q water. As well, just before collection began, the WWC collectors were run for approximately 10 minutes to ensure anything inside of the tubes was washed out before collection. All liquid effluent is captured in a 100mL sterile tubes and after collection all samples were immediately put on ice.

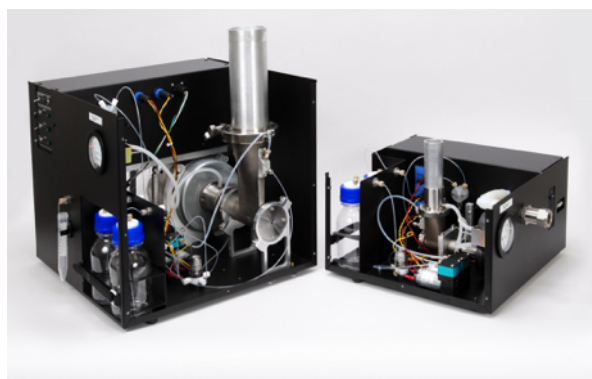


Figure 7: Open faced WWC's with a 1250 l/min unit on the left and a 100 l/min unit on the right.

### *III.4.2 Unmanned Aircraft System Collector*

The other collector used is a novel unmanned aircraft system (UAS), used to collect bioaerosols high in the atmosphere (Figure 8). It collects bioaerosols using the impaction method and is mounted on a hexacopter. A total of 37 inlet tubes are used to create a near laminar velocity of 20 m/s just before impaction, with an inducted fan creating the suction. The high velocity gives a calculated cutoff point of 0.181  $\mu\text{m}$ . The UAS utilizes two inlets with separate impaction plates to increase the total volumetric flow to 400 l/min and to give the user an option to load two different media in single run. The collection of bioaerosols on the UAS is completely autonomous, once the pilot flies to the desired capture location, the UAS capture system can be turned on remotely. The UAS will also collect data such as temperature, humidity, wind direction, and fan speed. Another important aspect is the ability of the UAS impaction inlets to face the wind at all times to increase collection efficiency. The total weight of the impactor is 1.83 lbs, which gives a flight time of approximately 20 minutes. The UAS could easily fly to 1,000 ft., but with FFA regulations, flight must stay under 300 ft. The impaction plates are covered with foil and sprayed with silicone spray just before a collection run. Bacteria will impact upon the foil and adhere to the silicone spray. Once a collection run is complete, the foil is removed and placed in sterile 100 mL tubes with Phosphate Buffer Saline (PBS) and shaken to remove the attached bacteria from the foil. All samples were immediately placed on ice after collection.

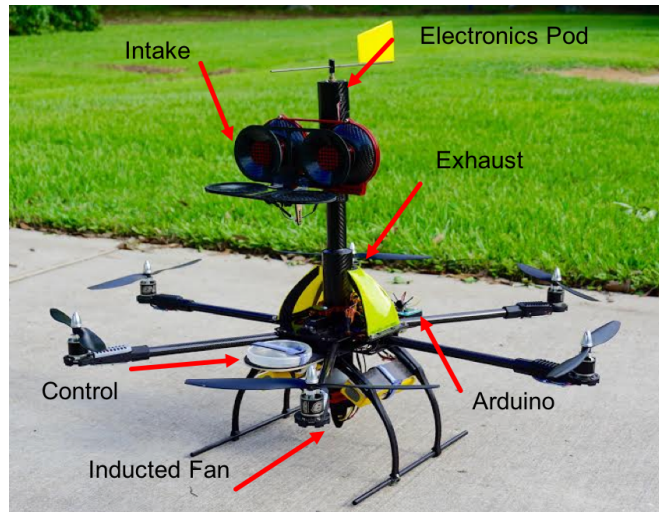


Figure 8: UAS collector, with intake doors open.

### III.5 Preliminary Test

The WWC was tested for its ability to collect *Salmonella* and keep the bacteria viable. The WWC was cleaned by first running ten percent bleach through the system, followed by isopropanol, and finished with Milli-Q water for a full 15-minute run. A fresh 30 mL batch of *Salmonella* was aerosolized using a collision air nebulizer pressurized to 20 psi. The WWC was run 4 different times, running for 15 minutes apiece, each sample issuing approximately 4 mL of collection fluid separately. The samples were immediately plated afterwards.

### III.6 Bioaerosol Analysis

STEC and *Salmonella* were confirmed by following the FSIS Microbiology Laboratory Guidebook, chapter MLG 4.08, adapting the sample processing for environmental sponges to air samples. To determine whether the amount of *Salmonella* and STEC collected from the air of slaughterhouse facilities is sufficiently large to be

detected by direct plating, an aliquot of the sample was spread-plated onto selective agar plates, incubated and enumerated if colonies were detectable. For qualitative analysis, all samples were processed within the same day of reception. One of the duplicate samples was tested using non-enrichment qPCR method using 16s rRNA based primers and STEC/*Salmonella* specific oligonucleotides [61-63] and the other was enriched and tested using an immunoassay method. Samples that tested positive were confirmed by conventional plating methods. From samples in locations of interest, DNA isolates were collected and sent to the Institute for Cellular and Molecular Biology at the University of Texas at Austin to delineate the microbiome of the collected samples using 16S rRNA-based Illumina Next Generation sequencing. This method allows for bacterial identification and taxonomy by comparing the 16S rRNA gene sequencing to differentiate organisms down to the species and subspecies level [64].

### *III.6.1 Plating*

The direct plating method was performed before and after enrichment of the sample by spread plating onto a thin layer of selective media that is overlaid with non-selective medium; this has shown greater recovery of sub lethal injured cells and an increase in number of organisms. The sample was plated onto a thin agar layer (TAL) media. During this process, after solidification of a selective medium in a petri dish (25 ml agar added to a height of 6mm), fourteen ml of melted TSA (44-48 °C) will be overlaid (7 ml/7 ml; two times overlay). The top layer, of a thickness from 3-4 mm, solidified and was either used or stored at a cool temperature until use. XLT-4 agar was overlaid with tryptic soy agar (TSA) to enumerate *Salmonella* counts. After sample spreading, the plates were incubated

at 35 °C for 24 hours. Once the 24 hour period had passed, the plates with typical colonies underwent further confirmation. In order to identify *Salmonella*, multiple biochemical and serological tests were carried out for at least three colonies. The run of tests includes Triple Sugar Iron Agar (TSIA), Lysine Iron Agar, and Urea test. Serological tests were completed using agglutination with *Salmonella* antiserum Poly a-z. Posse agar was overlaid with TSA to enumerate STEC colonies [65]. The plates were incubated at 35 °C for 24 hours after samples were spread. Once the 24 hours were up, colonies were tested for their biochemical properties using API 20E strip. The motility test was also performed, and the slide agglutination test using anti-O157 and flagellar H7 antiserum were performed. For qPCR, real-time PCR oligonucleotides were used [61-63]. For the immunoassay, analysis was conducted using a Crystal Diagnostics CDx system. However, with that said, none of the plating resulted in any pathogens.

### *III.6.2 DNA Extraction*

The Alkaline Lysis method was used to extract DNA from all the samples. The samples begin by centrifuging for five minutes and then adding 300 µl TENS. Afterwards, the sample was vortexed at a low speed for 20 seconds, upon which the samples are incubated for ten minutes at room temperature and then put on ice. Then the protein was precipitated by adding 150 µl 3N sodium acetate. The sample is then vortexed and centrifuged two minutes at 13,000 x g at 17 °C, at which point the supernatant is moved to a sterile 1.5 ml micro centrifuge tube. After the transfer, 10 µl of Poly Acryl Carrier (PAC) is added to every tube and inverted. Next, 1 ml of 100% isopropanol is added and the tubes are inverted ten times until well mixed and placed in the centrifuge for 20



minutes. The isopropanol was removed, leaving the DNA pellet in place. The pellet was then washed with 1 ml of cold, 100% ethanol and vortexed until the pellet releases from the bottom of the tube. The tubes are centrifuged for ten minutes and the supernatant is removed. Finally, the pellet is air dried and dissolved in 50  $\mu$ l of DNA hydration (Milli-Q water) solution. The DNA concentration was determined by measuring optical density ( $OD_{260}$ ) using a spectrophotometer (NanoDrop Technology, Wilmington, ED).

### III.6.3 qPCR

With the DNA successfully extracted, it was then added to PCR tubes containing PCR assay reagents and amplified in an automated thermocycler/analyzer. 3  $\mu$ l aliquots of the collected bioaerosols (for whole cell qPCR) or DNA extractions (for species specific qPCR) in appropriate dilutions are added as the DNA template to the PCR reaction mixture. This mixture consists of 5  $\mu$ l of 2 x Power SYBR Green PCR Master Mix (Applied Biosystems, Warrington, UK), 3  $\mu$ l of the hydrosol sample supernatant or DNA extract, 1  $\mu$ l Forward Primer and 1  $\mu$ l Reverse Primer sequences with sequences for virulence genes that are associated with pathogenicity of the strain, *stx* (Shiga toxin gene) and *eae* (Enteropathogenic E. coli (EPEC attaching effacing A gene) variants used for STEC, sequences of *invA* (genetic locus that allows *Salmonella* spp. To enter cultured epithelial cells) gene for *Salmonella*, and sequences for 16S rRNA (Table 1). The AB StepOne RT-PCR System (AB, Foster City, CA) is a thermo-cycling program that comprises of an initial cycle of 95  $^{\circ}$ C for ten minutes after which 40 cycles were run at 95  $^{\circ}$ C for fifteen seconds and 60  $^{\circ}$ C for 60 seconds. Once the PCR is completed, a melting curve is made for the temperature range of 60-90  $^{\circ}$ C to spot any non-specific



amplification, including primer-dimer induced positive results. The samples from PCR were cooled to 65 °C and then heated gradually by 0.2 °C/s to 95 °C. The DNA strand separation was specified by a big reduction in fluorescence at the melting point. Fluorescence signals that were obtained were used for continuous monitoring to confirm amplification specificity [66].

Table 1. Sequence of specific and 16S rRNA oligonucleotides used in the study.

<b>Primer Name</b>	<b>Sequence</b>	<b>Amplicon (bp)</b>
<i>Stx</i> F	5' TTT GTY ACT GTS ACA GCW GAA GCY TTA CG 3'	132
<i>Stx</i> R	5' CCC CAG TTC ARW GTR AGR TCM ACD TC 3'	
<i>Eae</i> F	5' CAT TGA TCA GGA TTT TTC TGG TGA TA 3'	102
<i>Eae</i> R	5' CTC ATG CGG AAA TAG CCG TTM 3'	
<i>invA</i> 139 F	5' GTGAAATTATCGCCACGTTTCGGGCAA 3' (287-312)	284
<i>invA</i> 141 R	5' TCATCGCACCGTCAAAGGAACC 3' (571-550)	
16S 1369 F	5' CGG TGA ATA CGT TCY CGG3'	123
16S 1492 R	5' GGT TAC CTT GTT ACG ACT T3'	

The number of cells in a sample is proportional to the threshold value of DNA quantification, defined as Ct, which depends on the total number of DNA in a sample. The threshold value is used to relate the logarithm of bacteria concentration in a sample linearly, with higher values of Ct associated with smaller values of concentration. King and McFarland used fresh dilutions of *E. coli* stock suspensions to create a standard

calibration curve for each analysis and was also used here [60]. The mid-log *phase E. coli* stock suspensions contained fresh cells that had not been exposed to stress, and on the basis of the LIVE/DEAD<sup>®</sup> BacLight<sup>™</sup> Bacterial Viability Kit (Invitrogen Molecular Probes, Carlsbad, CA) staining results of the stock suspensions, the number of culturable cells were directly proportional to the total number of cells in a ratio of at least 90%. Each test or calibration data point showing the relationship of Ct as a function of microorganism concentration was based on three replicate tests. The least square best fit for a typical calibration curve is:

$$Ct = -1.35 \ln(C_{CFU}) + 34.1$$

where cCFU is equal to CFU/ml. In applying the calibration curve to a sample, a reading Ct would be obtained from the instrument and the corresponding cell concentration would be calculated by rearranging to:

$$C_{CFU} = e^{\left(\frac{34.1-Ct}{1.35}\right)}$$

The DNA of samples located in positions of interest were sent to the Institute for Cellular and Molecular Biology at the University of Texas at Austin.

### **III.7 Computational Fluid Dynamics**

Blueprints were collected from each facility after bioaerosol collection was complete. The facilities were modeled in SolidWorks according to their floor plans. The HVAC systems were also modeled using the information from the mechanical blue prints. The exact positions of the collection sites and locations of importance were found and labeled in the models. The airflow inside the facilities was modeled using SolidWorks Flow to match the HVAC design of every facility. Experimental collection sites were correlated

with the airflow by simulating the intakes of the WWC collectors at each experimental site for particle collection. Other metrics were analyzed such as velocity profiles, contaminant removal effectiveness, and local mean age of air. Particles were simulated appearing from cattle hides, the main source of pathogens and other bioaerosols. The sizes of particles were varied from 1  $\mu\text{m}$  to represent a single bacterium, to 8  $\mu\text{m}$  to represent a coagulation of particles. Particle spread from the model was analyzed in accordance with experimental sampling times. The release of particles began upon the introduction of the first cattle and increased as more cattle were introduced. Then, new HVAC models were created around the facilities layout to create an optimized airflow pattern that would inhibit the spread of bioaerosols. Steady state systems were used for all models.

### *III.7.1 Facility A*

The dual intakes of Facility A output air at 102.33  $\text{ft}^3/\text{s}$  each. The ceiling exhausts range from 41.67 to 70  $\text{ft}^3/\text{s}$  and create a total negative pressure in the slaughtering room, causing airflow to return to the room through fly fans. Workers and cattle carcasses were modeled as rectangular prisms with an equivalent surface area of 20  $\text{ft}^2$  and 67.6  $\text{ft}^2$ , respectively. Heat generation was also included in the model with workers giving off 330 BTU/h and the cattle carcass at the bleeding position giving off 4400 BTU/h. Heat generation from the carcass was not considered after the bleeding pit. The 190 °F water used to wash the saw for spine splitting was modeled to emit 1,583 BTU/h. The total volume of the facility was 76,840  $\text{ft}^3$ . The total mesh consisted of 3,799,238 cells and took nineteen hours to complete 1,205 iterations. The air coming through the intakes was not measured during collection experiments, and was set to 60 °F with fully developed

flow. The initial temperature of the system was set to the average found in the facility of 68 °F. For the particle studies, all particles are set to an initial velocity of 0 ft/s and an initial temperature of 68 °F. Particle traces were created to simulate bioaerosol release from the cattle carcasses during processing. First, 100 evenly spaced particles were released for fifteen minutes from the modeled carcass at the bleeding pit. Then, as the next carcass enters and the previous moves to the de-limbing area, 100 particles are released from the carcass at the bleeding pit and at the de-limbing process. As the third carcass enters and the other two move down the processing line, 100 particles are released for from the bleeding pit, the de-limbing area, and the de-hiding process. Particles are not released from carcasses after the de-hiding process. As well, 20 particles were released from the entryway from the main hallway to the slaughter floor facility to simulate workers entering the facility. This process was run twice for particles of 1 and 8  $\mu\text{m}$ .

### *III.7.2 Facility B*

This rural facility did not have an exhaust or an intake inside the slaughtering room, instead a single fan was located near the entry door, facing the knocking pen. The fan was modeled to eject air at 16 ft/s. The entry door was open during the entire slaughtering process, and is modeled as a static pressure boundary layer. The same measurements for workers and cattle are used as previously stated. The total volume of the facility was. The total mesh size was 2,550,639 cells with a total of eleven hours to complete 1,032 iterations. The initial temperature of the room was set 68 °F. All particles initially had the same temperature as the fluid inside the facility and an initial velocity of 0 ft/s. Akin to Facility A, particles were released from cattle carcasses to simulate the process during

experimental collection, however, only two positions were used because the de-limbing and de-hiding occurred in the same position. First, 100 particles were initially released from carcass in the bleeding pit. Then, 100 particles were released from the de-limbing/de-hiding carcass. This process was run twice for particles of 1 and 8  $\mu\text{m}$ .

## CHAPTER IV

### RESULTS AND DISCUSSION

#### IV.1 Facility A qPCR Analysis

The bioaerosols collected during the three-day period at Facility A were categorized into Total Bacterial Count (TBC), STEC, and *Salmonella* concentrations in operational taxonomic units (OTUS) per m<sup>3</sup>. The concentrations of STEC are listed in two separate categories corresponding to the two different primers used for qPCR, *stx* and *eae*, respectively. These were further categorized into their collection location, time of collection, distance from collection, and number of workers present. As only qPCR was used to enumerate bacteria counts, further analysis such as Illumina Sequencing needs to be performed to verify the quantities of bacteria. The log TBC collected each day was calculated and plotted on Figure 13. The most bacteria were collected on the third day with a log TBC of 4.9 and the least amount of bacteria were collected on the second day with a log TBC of 5.7. There was no significant relation found between consecutive collection days and increasing bioaerosols.

As well, the log *Salmonella*, STEC with *eae* primers, and STEC with *stx* primers were plotted along with consecutive collection days (Figures 9). Aerosolized *Salmonella* was found to significantly increase linearly between consecutive days. The least amount was collected on the first day with log 6.9 and the most was collected on the last day with counts of log 10. No correlation was found with consecutive days and total amounts of collected STEC processed with the *stx* primer. The largest amount of STEC was collected

on the final day with log 5.5 OTUs/m<sup>3</sup> and the least amount was collected on the second day with log 4.4 OTUs/m<sup>3</sup>. However, with regards to STEC analyzed with the *eae* primer, a positive exponential correlation was found. As consecutive days passed, the concentration of aerosolized STEC increased exponentially. The lowest concentration was collected on first day and the highest was collected the last day, log 1.3 and log 4.5 respectively. There was no statistical difference between concentrations of STEC *stx* and STEC *eae* collected each day using an ANOVA single factor. It may be inferred that the HVAC system is not properly designed to move air in a single direction, and instead spreads the air around the entire facility, allowing the pathogens to find niches and survive to be re-aerosolized the next day.

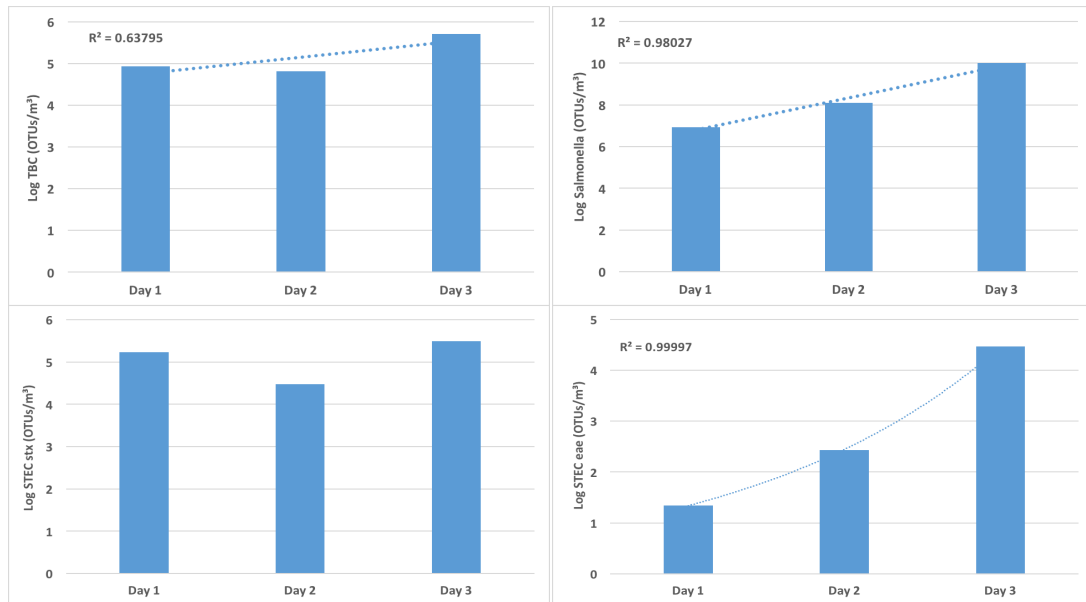


Figure 9: TBC, STEC, and *Salmonella* collected each day. (Top Left) Log TBC collected each consecutive day at Facility A. The most bioaerosols were captured on the last day, while the least amount of bioaerosols were captured on the second day. No significant relationship was found between consecutive days and increasing bioaerosol counts. (Top Right) Total log concentrations of *Salmonella* collected each day. *Salmonella* concentrations increase linearly each day. (Bottom Left) Total log concentrations of STEC collected each day analyzed using *stx* primers. (Bottom Right) Total log concentrations of STEC collected each day analyzed using *eae* primers. STEC *eae* concentrations increased exponentially each day.

It is known that humans shed bacteria which becomes aerosolized and has the ability to increase the bioaerosol concentrations in a room. During every collection period in Facility A, the number of workers present was documented. The exact movements of the workers were not tracked, but the general movement was noted and found that most of the workers ended up moving down the entire production line from the bleeding pit down to the spine splitting station. The amount of workers sometimes varied between morning and afternoon phases. It appeared that the concentration of aerosolized bacteria increased with the number of workers present, but no significant correlation was found between the number of workers and the log TBC (Figure 10). Many more data points are necessary to see if there indeed exists a trend. As well, a single factor ANOVA test revealed that neither of the populations are significantly different. Another important aspect of bioaerosol collection is the distance of the collector from the site of importance, in the case of this study, the carcass. If the WWC was placed too close to the carcasses, it would get in the way of the workers and would likely become damaged from the amount of water being sprayed in the areas directly around the carcass. Therefore, the distance of each collector from the hide was measured and plotted with the TBC collected at the corresponding location (Figure 10). No correlation was found between the distance of the collector from the hide and TBC. It is likely that there are too many other factors changing the concentration of bacteria, such as local air velocity and the time of collection, for the distance of the collector from the hide to have a significant relationship.



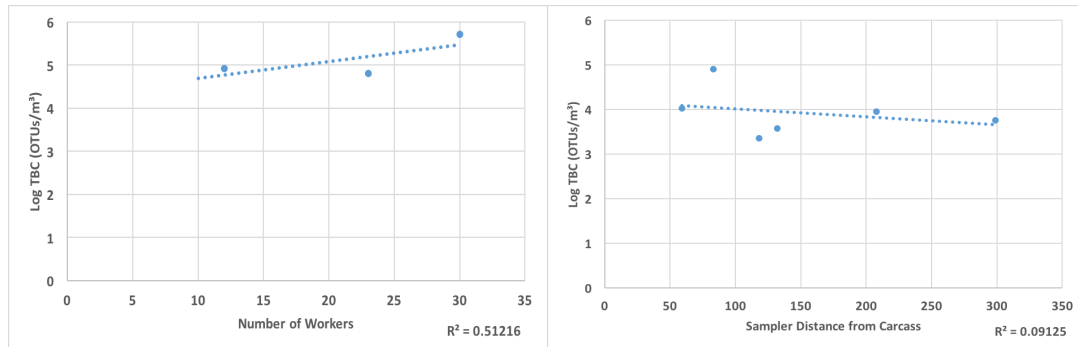


Figure 10: Workers and WWC distance compared to TBC. (Left) The log TBC collected each day with the corresponding average of workers present that day. No significant relationship was found between TBC and number of workers. (Right) The log TBC collected at each sampling location with the corresponding distance from the carcass. No significant relationship was found between TBC and the distance from the carcass.

A representation of a bad HVAC design could be realized if aerosolized bacteria concentrations increase throughout the day. As each new beef cow is introduced, more bacteria are introduced as well. A HVAC system with low air exchange rates will not be able to keep up with each new iteration of bacteria populations brought in from the cattle. TBC were averaged over each of the three collection days during the morning and the afternoon phases (Figure 11). The average concentration collected in the morning and afternoon was log 4.46 and log 5.38, respectively. The concentration of bioaerosols collected in the afternoon was significantly larger than the morning. If the facility turns off the main intakes between production runs in the morning and afternoon, the aerosolized bacteria will mainly be effected by gravity, therefore, their airborne time is dependent on their vertical height in the facility and their settling velocity. If a  $1 \mu\text{m}$  bacterium is twenty feet high it will take the particle 154 hours to reach the ground. An agglomeration of particles with an aerodynamic diameter of  $8 \mu\text{m}$  will reach the ground in 2.8 hours. This means with the time between the end of the morning phase and the afternoon phase being

approximately 1.5 hours, the bacteria brought in from the morning cattle will still be airborne by the time the next phase begins. Also, between phases the facility exchanges air fourteen times, if the air intakes are not turned off. With bacteria increasing in the afternoon, we can safely assume the HVAC system is not removing bioaerosols effectively at all. *Salmonella* concentrations were averaged during the morning and afternoon phases (Figure 11). Although more *Salmonella* was collected during the afternoon, there was no significant difference between morning and afternoon. An average of log 9.48 was collected in the morning, and an average of log 9.81 was collected in the afternoon. As well, no significant differences were found in STEC concentrations analyzed with the *stx* primer for the morning and afternoon phases (Figure 11). The concentrations were higher in the afternoon. The concentration of STEC *stx* was log 3.75 in the morning and log 4.3 in the afternoon. This is a very large concern for beef slaughter facilities. STEC is a deadly pathogen and these results show that the processing in the facility actually becomes more dangerous throughout the day. On the other hand, STEC isolated with the *eae* primer had greater concentrations in the afternoon, but it was not significantly different (Figure 11). An average of log 2.675 was collected in the morning, and an average of log 3.67 was collected in the afternoon.

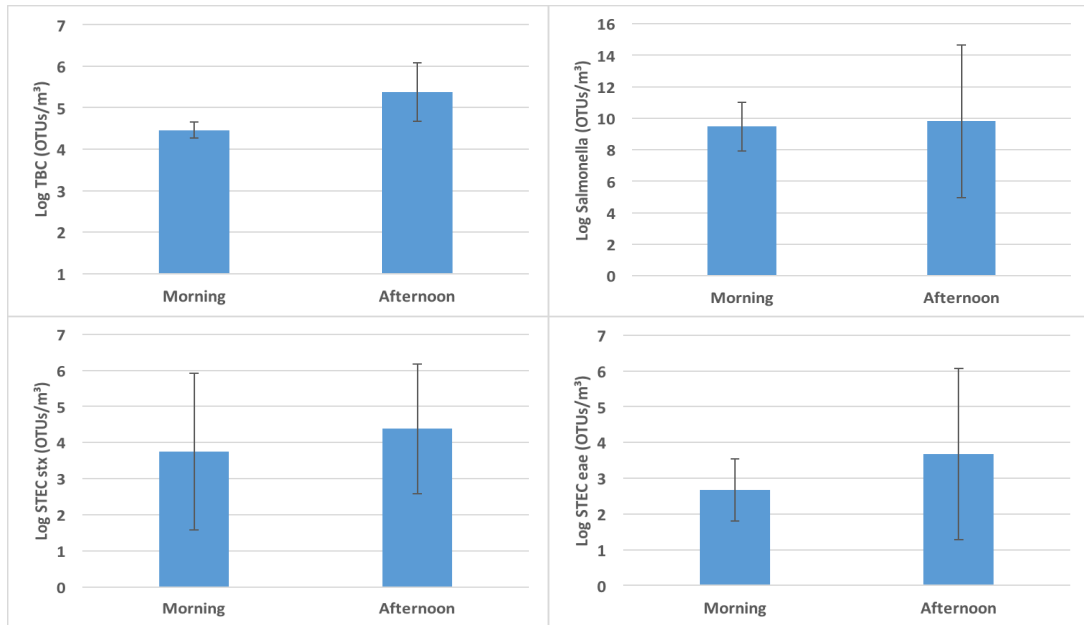


Figure 11: TBC, *Salmonella*, and STEC collected in the morning and afternoon. (Top Left) Log TBC collected during morning and afternoon phases. The concentration of bioaerosols was significantly larger in the afternoon. (Top Right) Log *Salmonella* collected and averaged during morning and afternoon phases. The concentration of *Salmonella* was not significantly different between the two phases. (Bottom Left) Log STEC *stx* collected and averaged during morning and afternoon phases. (Bottom Right) Log STEC *eae* collected and averaged during morning and afternoon phases. The concentration was not found to be significantly different between morning and afternoon.

Bioaerosol samples collected at each location within Facility A were averaged and plotted in Figure 12. The locations of sampling include continuous WWC near de-hider, continuous WWC near freezer, dynamic sampler bleeding pit, dynamic sampler de-limbing, dynamic sampler de-hiding, and dynamic sampler spine splitting/washing. The most bioaerosols were collected during the de-limbing process, right before the de-hiding process, with a log 4.9 TBC. Contrary to other studies, the least amount of bioaerosols were collected at the de-hiding process, with a TBC of log 3.35. All of the standard deviations overlap between samples, however, a one-way ANOVA showed that there is a significant difference between at least one of the samples. Using a t-test assuming unequal variances, it was found that the bleeding pit was significantly different ( $P < 0.5$ ) than the

sampler near the freezer. This result is expected because the freezer is at the rear of the facility and the bleeding pit is at the front. As well, the continuous sampler near the de-hider was significantly different ( $P < 0.5$ ) from the bleeding pit. This is likely due to the fact that the continuous sampler near the de-hider had higher velocity air flow coming directly from the HVAC system, blowing bioaerosols in its direction. The bioaerosol concentrations collected between the dynamic de-hider and the continuous de-hider were also significantly different. Again, this is likely because the continuous de-hiding sampler had the direct stream of the HVAC intake pointed towards it. Continuing, the bleeding pit was significantly different than the de-limbing area. The most bioaerosols were collected at the de-limbing process, with a concentration of log 4.9. The same process was used for *Salmonella* concentrations found at each location in Facility A and the distribution (Figure 12) is very similar to the TBC distribution in Figure 23. The largest *Salmonella* concentration was collected during the de-limbing process and the least was collected at the de-hiding process with concentrations of log 9.23 and log 6.37, respectively. A one-way ANOVA test revealed that none of the collection sites are significantly different with respects to *Salmonella* concentrations. STEC that was analyzed using the *stx* primer also had no significant differences between collection sites (Figure 12) using the ANOVA test. The highest concentration of STEC *stx* was collected at the spine splitting/washing stage with a concentration of log 4.3, while none with the *stx* primers were collected at the continuous WWC near the freezer. This is an interesting result since these two locations were fairly close to each other with respects to the other collection sites. It may be that there are different STEC strains present that exhibit the *eae* but not the *stx* gene. Larger

sample sizes are needed in the future. Similarly, the STEC analyzed with the *eae* primer also had no significant differences between collection sites (Figure 12). The most was collected near the freezer with log 3.35 and no STEC *eae* was collected at the bleeding pit and the de-hiding process. It is interesting that no STEC *stx* was found near the freezer, but the most STEC *eae* was found there. This may be explained by the *E. coli* strain diversity. The majority of enteropathogenic *E. coli* (EHEC) strains harbor both *stx* and *eae* genes, but some *eae*-negative STEC strains, such as O91:H21 and O113:H21 strains, which cause bloody diarrhea and HUS in humans, have been described previously [66]. Similarly, the *E. coli* strains can be *stx* negative but *eae* positive [67]. The *stx* gene that is encoding Shiga toxin (Stx) is carried by a bacteriophage. During infection or culturing of the strain, the loss of the Stx-encoding bacteriophage may occur. Because of the presence of the *eae* gene but lack of the *bfpA* gene, the *stx*-negative isolates are considered atypical enteropathogenic *E. coli* (aEPEC). As detection of STEC infections is often based solely on the identification of the presence of *stx* genes, these may be misdiagnosed in routine laboratory testing, requiring improved diagnostic approach for the detection, treatment, and ultimately, prevention of these potential pathogens [67]. It should be noted that the qPCR data requires further analysis, such as Illumina Sequencing, in order to truly verify the quantities of bacteria collected.

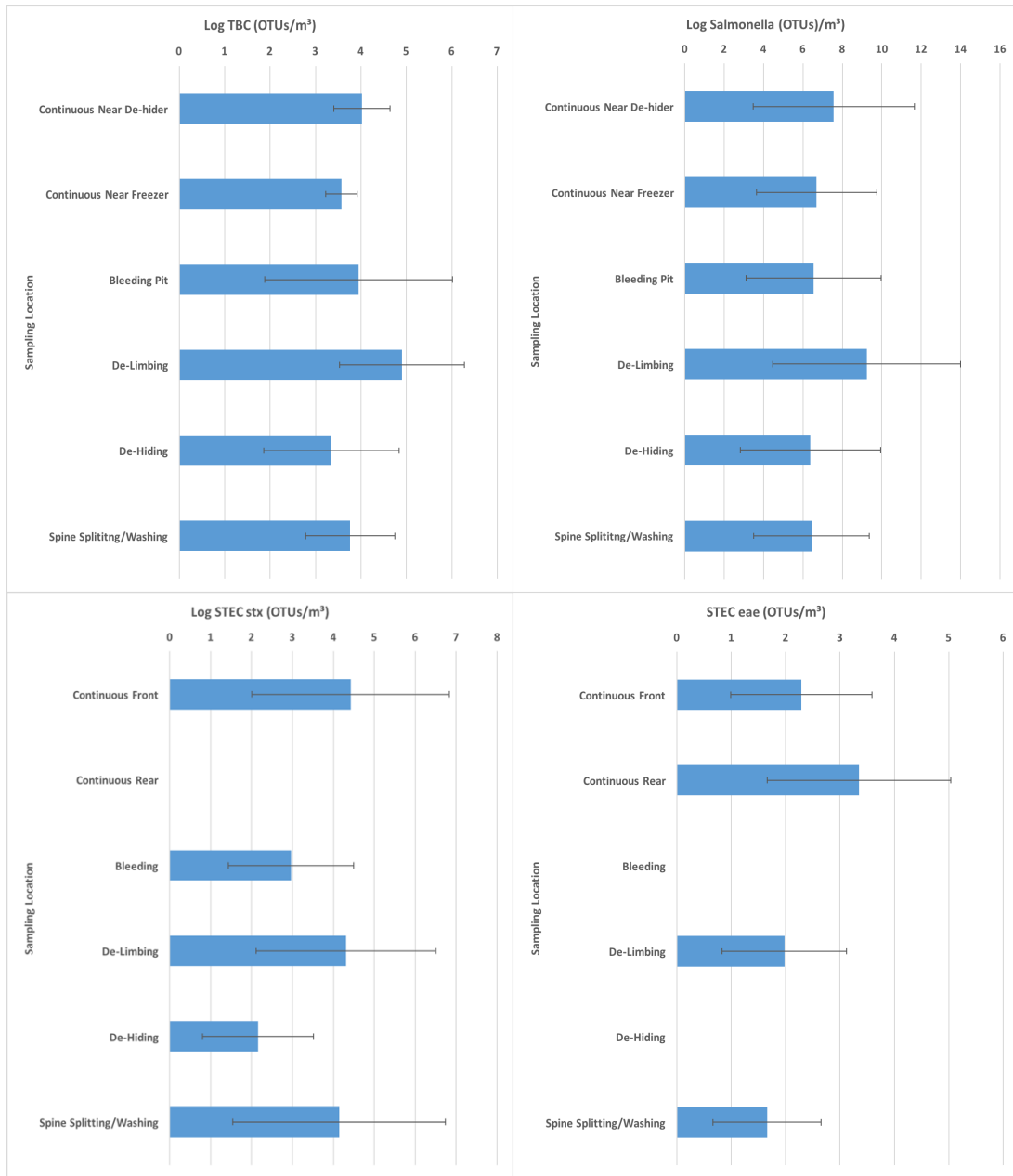


Figure 12: TBC, STEC, and Salmonella collected at each site. (Top Left) Average concentrations collected at each location in Facility A with a sample size of six. The bleeding pit was significantly different from the de-limbing, near freezer, and the de-hiding area. The continuous WWC near the de-hider was also significantly different than the de-hiding area. (Top Right) Average concentrations collected at each location in Facility A with a sample size of six. None of the collection sites had significantly different amounts of *Salmonella*. (Bottom Left) Average concentrations of STEC *stx* collected at each location in Facility A with a sample size of six. None of the collection sites had significantly different amounts of *Salmonella*. (Bottom Right) Average concentrations of STEC *eae* collected at each location in Facility A with a sample size of six. None of the collection sites had significantly different amounts of *Salmonella*.

Temperature and humidity has been found in the past to play a heavy role in the concentrations of aerosolized bacteria [67, 68], however, there was no significant correlation found in this study.. The two Hobo units, placed on top of both continuous WWC samplers, measured temperature and humidity during the entirety of collection in Facility A. The temperature and humidity was averaged during the morning and afternoon phases of production in the facility. Figure 13 displays the average temperature and humidity during each collection phase along with the TBC. Although there seemed to be a trend between increasing temperature and decreasing TBC, there was no strong relationship. A larger sample size would need to be collected in order to test for a strong relationship.

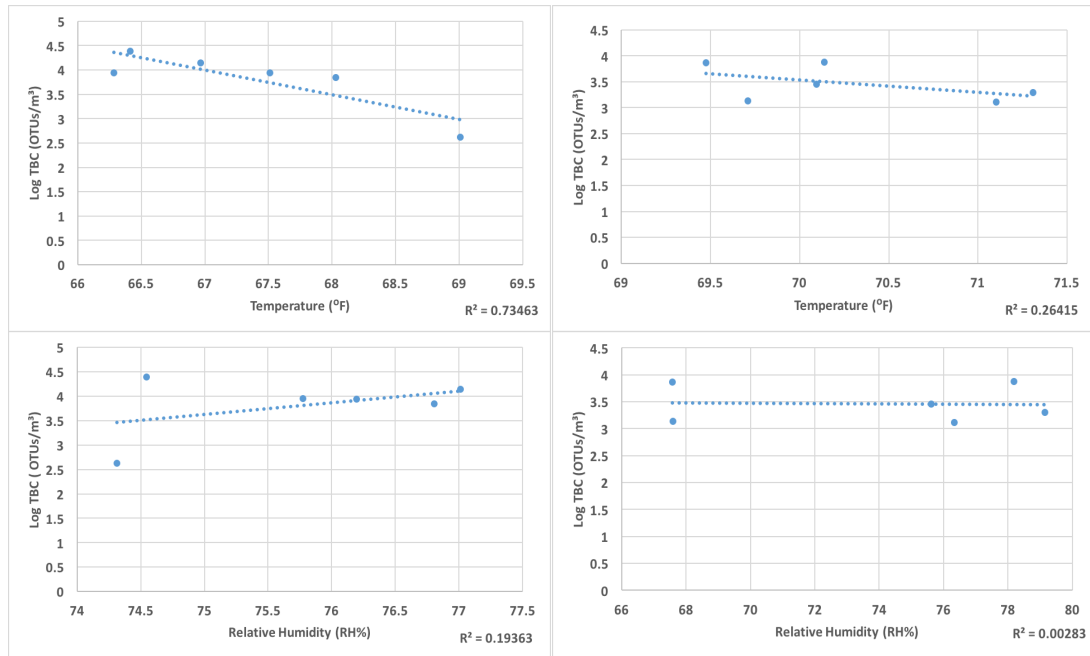


Figure 13: TBC compared to temperature and humidity. (Top Left) TBC and temperature collected from the continuous WWC near the de-hider during morning and afternoon phase at Facility A. No correlation was found between temperature and the TBC. (Top Right) TBC and temperature collected from the continuous WWC near the freezer during morning and afternoon phase at Facility A. No correlation was found between temperature and the TBC. (Bottom Left) TBC and humidity collected from the continuous WWC near the de-hider during morning and afternoon phase at Facility A. No correlation was found between humidity and the TBC. (Bottom Right) TBC and humidity collected from the continuous WWC near the freezer during morning and afternoon phase at Facility A. No correlation was found between humidity and the TBC.

The temperature measured near the de-hider was significantly lower than the temperature near the freezer during all three days (Figure 14). This is most likely due to the fact that the two intakes for the HVAC system had their airflow directed straight towards the de-hiding area. The temperature was highest on the second day and the averages each day varied from 66.3 to 71.2 °F, however the maximum and minimum temperature variation was a bit larger, from 65.2 to 74.1 °F, resulting in a 5.8% total deviation in temperature. The humidity near the de-hider was significantly different the first day of collection, but was not significantly different the next two days of collection (Figure 14). Humidity varied widely in Facility A due to the use of high pressure hoses,



water baths, and sinks with temperatures near 180 °F that produced a lot of steam. The average relative humidity varied from 67.6% to 79.1%, however, the maximum and minimum humidity variation was much larger, from 49.4% to 95.89%, resulting in a 47.4% total deviation in relative humidity. This result shows that although the facility managed to regulate temperature well, it was not capable of controlling the humidity level very well. This is mostly due to the hot water baths and hoses used to sterilize equipment and spray floors. Although ambient temperature was not logged from outside the facility, average weather data was taken from the KCLL weather station. When graphed with the average humidity and temperature data logged from inside the facility during each day, it appears there is a relationship, however, not enough data points are available to be sure (Figure 14). Temperature should be logged outside the facility during the duration of testing in order to truly see if outside temperature is having a large effect on the temperature and humidity control in the facility.

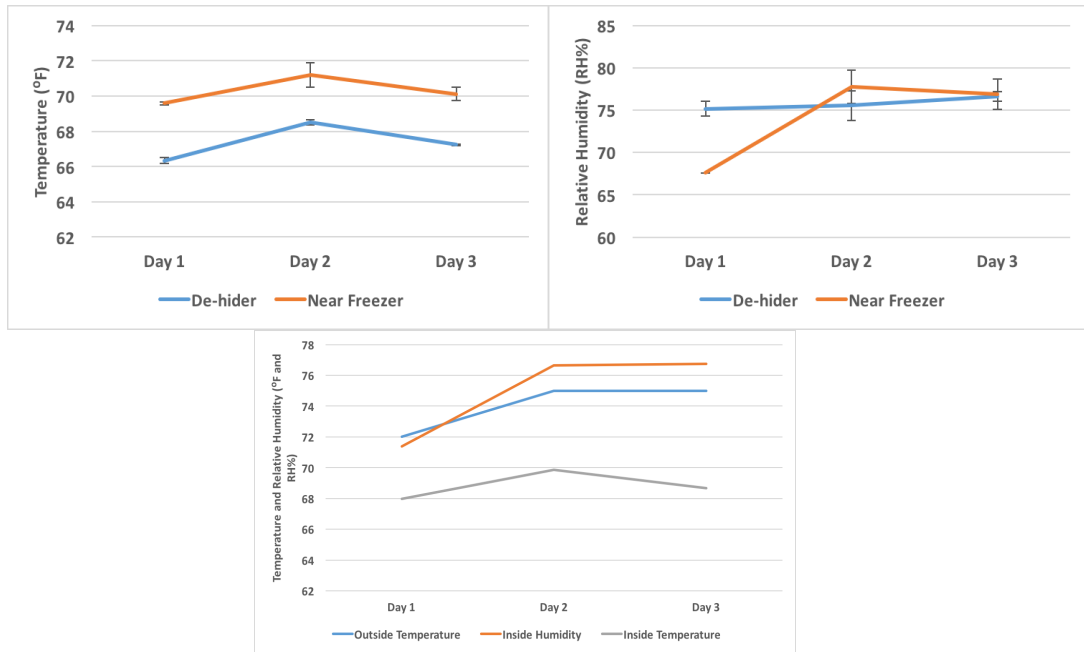


Figure 14: Temperature and humidity compared inside the facility. (Top Left) Temperature was measured with Hobo units and averaged each day at the continuous WWC units near the de-hider and the freezer. The temperature difference between the two areas is significantly different. (Top Right) Humidity was measured with Hobo units and averaged each day at the continuous WWC units near the de-hider and the freezer. The humidity difference between the two areas was only significantly different the first day. (Bottom) Outside temperature seems to be related to the temperature and humidity inside Facility A. More data points are needed in order to determine if there is a positive relationship.

The feedlot belonging to Facility A was tested with a dynamic WWC alongside the novel UAS collector. The collectors were both placed downwind of the cattle, and the wind was strong at 20 mph due northeast. The temperature was 75 °F and the relative humidity was 78%. The samples were collected at 5:00 P.M. The UAS collector performed extraordinarily well, capturing a large TBC count (Figure 15). The UAS utilizes a negative feedback control between a rotary encoder and a servo to allow the intakes to face the wind at all times. It is very likely that this ability allowed the UAS the capture more bacteria than the WWC that day. Much more testing and larger sample sizes are needed to confirm the efficiencies of the UAS collector. However, both collectors

captured similar concentrations of STEC, analyzed with the *stx* primer (Figure 15). *Salmonella* nor STEC analyzed with *eae* were found. More days of testing are needed as well as testing at different times of day and different conditions. The concentrations of STEC are likely greater than the TBC because of the supercoiling that can occur with DNA.

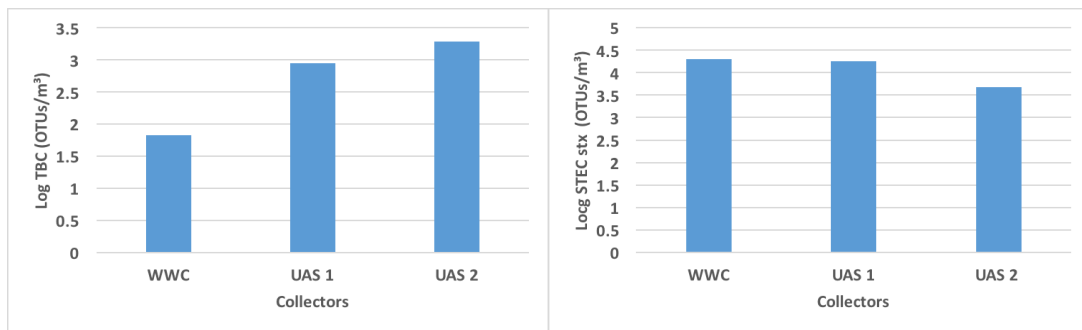


Figure 15: TBC and STEC collected in feedlot belonging to Facility A. (Left) TBC collected from the UAS and WWC in Feedlot belonging to Facility A. (Right) STEC *stx* collected from the UAS and WWC in feedlot belonging to Facility A.

## IV.2 Facility A CFD Analysis

### IV.2.1 Original Design

The incoming air from the dual intakes form loose vortices in the front and rear of the facility (Figure 16). The intakes, high on the wall, direct air at an angle across the facility towards the floor (Figure 17). The intake closer to the front of the facility shoots its air almost directly at the de-hiding process, which is the process that causes the most aerosolization of bacteria according to other studies. The primary mixing is caused by this intake and is noticed when the top intake flow trajectory is isolated (Figure 18). This type of mixing causes bioaerosols to be spread from the front to the rear of the facility,

endangering people who consume the final product. Once the airflow escapes the loose vortices formed at the front of the facility, the airflow travels underneath the intakes into the vortices at the rear of the facility. As well, the direction of the vortices at the rear of the facility is particularly dangerous because the velocity vectors stream towards the freezer door, possibly allowing many bioaerosols to enter whenever it is opened. The local mean age of air (LMA) at head level displayed in Figure 19 describes the latency of air in the facility. The area at the front of the facility near the knocking pen has very slow air movement. The center of both vortices in the front and rear of the facility are noticed as well. These locations could become areas of particle deposition. The location of the dynamic WWC collector at the de-limbing area was inside the vortices at the front of the facility and could describe why it collected the highest concentration of particles. The quickest air currents, apart from immediately after the intake, occur around the de-hiding area and most likely gives significant aid in spreading the bioaerosols off the hide of the cow. Temperature at head level in the modeled facility agrees with the experimental data in that the air is colder near the de-hider than the air near the freezer (Figure 20).

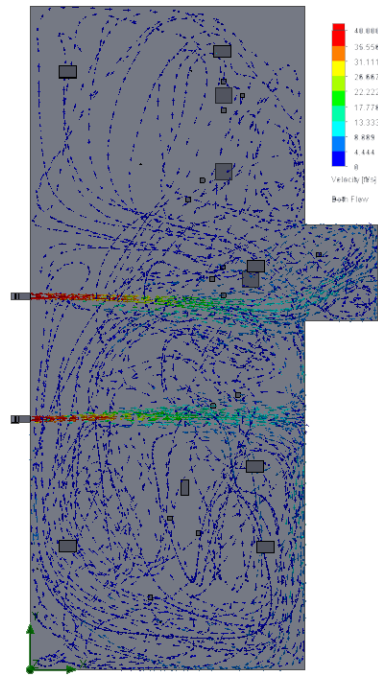


Figure 16: Skyview of the flow trajectory in Facility A created by dual intakes emitting air at 102.33 ft<sup>3</sup>/s. Loose vortices form in the front and rear of the facility. The air becomes well mixed throughout the facility.

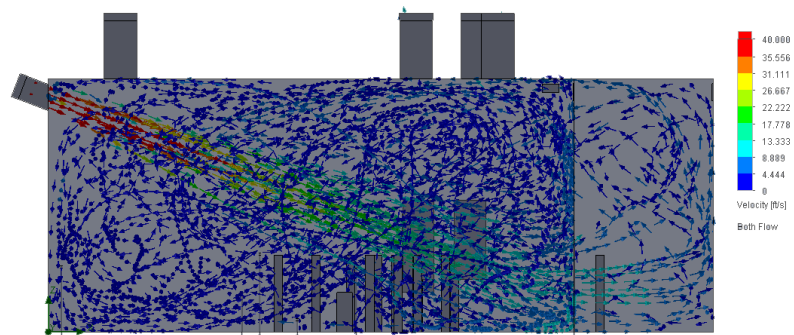


Figure 17: Side view of flow trajectories from the dual intakes in Facility A. The angle of the intakes causes the air stream to flow right next to the de-hiding area.

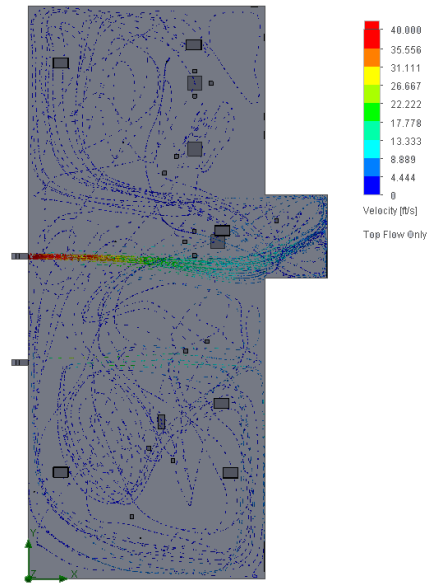


Figure 18: The isolated flow trajectory of the intake closer to the front of the facility. This intake causes the most particle spread throughout the facility due to the nature of its trajectory passing through the de-hiding process.

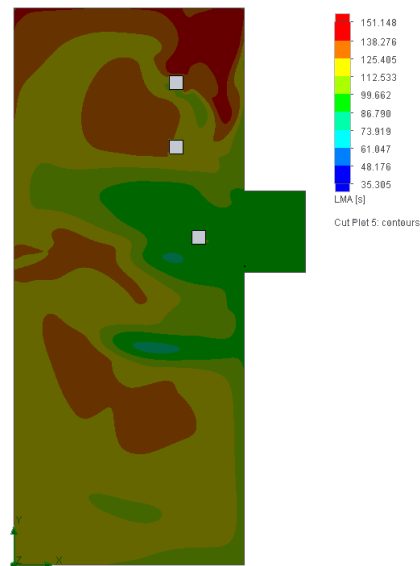


Figure 19: The LMA at head level in Facility A. The slowest air movement is in the knocking pen where the cattle enter the facility. The quickest air movement is in the de-hiding area.

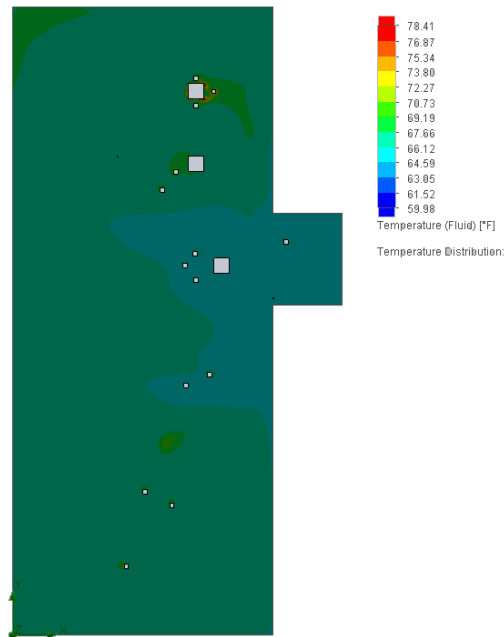


Figure 20: Temperature distribution of air inside of Facility A. The coldest region of air is around the de-hiding area.

Velocity point profiles were taken from each location of the WWC inlets to discover if the local velocity profiles and LMA were affecting the concentrations of bioaerosols collected. The velocity magnitudes can be clearly seen in Figure 21. Generally, a high velocity around the inlet of a bioaerosol collector will cause less total bacteria to be collected. The highest velocity magnitude belongs to the area near the continuous WWC near the de-hider, however, this WWC collected the second highest concentration of bioaerosols. It is likely that in this case the higher velocity is offset by the large number of bacteria that are being aerosolized from de-hiding process. The intakes airflow stream directs the air straight from the de-hiding process towards the continuous WWC. If the continuous WWC de-hider is taken from the data set, the general trend shows that less bioaerosols are collected when the velocity magnitude is higher. Furthermore, the de-

limbing area, responsible for the highest bacterial concentration, had the largest negative velocity vector, -0.13 ft/s, in the z-direction. A negative velocity profile in the z-direction will greatly aid the WWC's in collecting bioaerosols. A positive velocity in the z-direction will cause more bioaerosols to move past the inlet of a collector, such as the case with the de-hiding area, which had the largest positive velocity vector in the z-direction of 0.6 ft/s. The LMA of the de-limbing area was 326 s, meaning this location had the highest latency of air compared to the other collection locations. These two factors are likely to be the reason for the dynamic WWC near the de-limbing area to have collected the highest concentration of bioaerosols, and gives credence to the model of Facility A.

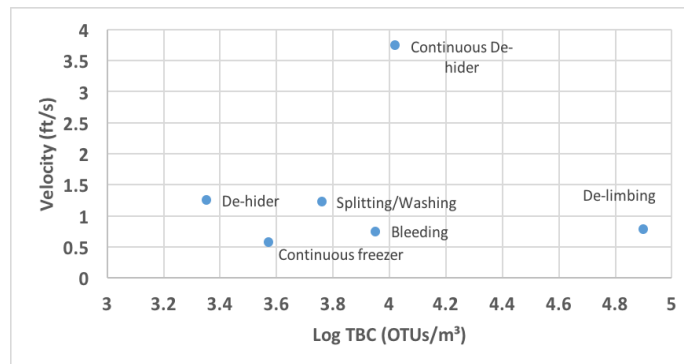


Figure 21: Velocity magnitudes at each collector location plotted with the log TBC.

Particle trace analysis was conducted to simulate bioaerosols emitting from the hide of the carcasses. A total of one hundred particles were released from the carcass at the bleeding pit (Figure 22). The backdraft created from the vortices caused the particles to immediately flow towards the rear of the facility. While some particles are carried back



into the cyclone by the intake near the front of the facility, many travel underneath the intakes air current and enter the vortices at the rear of the facility. Once at the rear of the facility, the particles have a high likelihood of entering the chiller.

Next, particles were released from the bleeding area as well as the de-limbing area, numbering 200 (Figure 22). Besides the overall change in concentration, the only main difference is the local concentration of particles that remain around the de-limbing process due to low velocity in that area. Finally, 300 particles were released from the bleeding, de-limbing, and de-hiding area (Figure 22). The only real difference is the change in concentration of particles. During this time, the dynamic WWC was collecting at the de-hiding area. Due to its position underneath the intake airflow, it collected the least amount of bioaerosols. While the facility was processing cattle, workers would walk regularly in and out of the doorway separating the slaughter floor from the main hallway. Particle studies were run to simulate a person entering the facility from the hallway. Continuing the trend of the other particle studies, the particles travelled throughout the entire facility (Figure 23). No major difference was found in the traces of the 8  $\mu\text{m}$  compared to the 1  $\mu\text{m}$  particles. However, there was a difference in contamination removal effectiveness (CRE), defined as the concentration of particles in the exhaust divided by the mean concentration in the room. The CRE was 89% for particles measuring 1  $\mu\text{m}$  and dropped efficiency by 5% for particles measuring 8  $\mu\text{m}$  during a one-hour period. Although the CRE was not altogether bad, it is not a good measurement in this case for factory cleanliness because the particles spread across the entire facility and had ample time to adhere to surfaces. Seedorf and Hartung found that 6.1 colony forming units (CFUs) of

Enterobacteriaceae emit per hour per 500 kg of cattle weight [69]. With a black Angus cow weighing about 1,800 lbs, this amounts to 2,054,566 enterobacteriaceae emitted from a single cow in an hour, or, 571 in a second. With a processing time of 1 hour and 30 minutes, and four cattle processed introduced step-wise, that leaves 925,020, or 425 per m<sup>3</sup>, remaining in the facility, emitted from cattle alone.

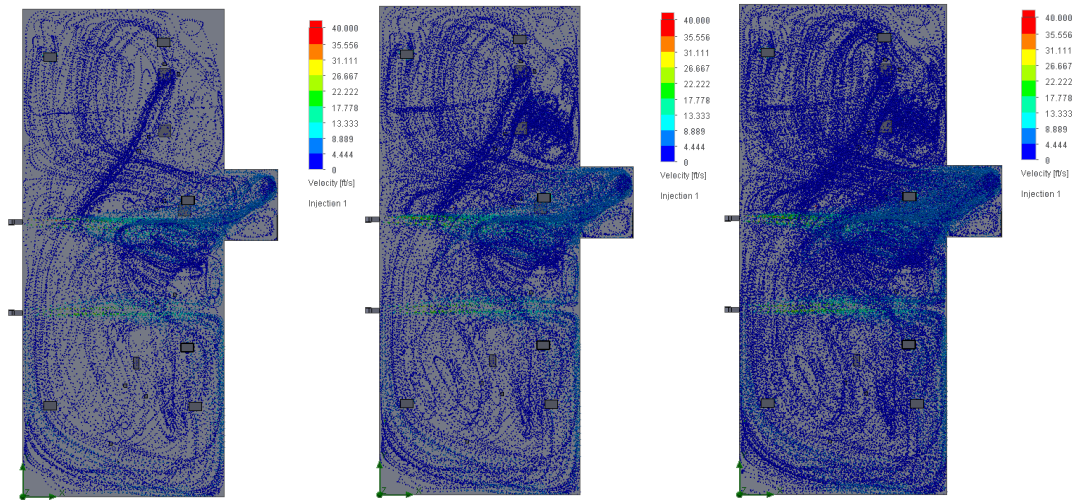


Figure 22: Skyview of particles released in Facility A. (Left) Skyview of Facility A when 100 particles are released from the carcass at the bleeding pit. (Middle) Skyview of Facility A when 100 particles are released from carcasses in both the bleeding pit and the de-limbing area. (Right) Skyview of Facility A when 100 particles are released from carcasses in the bleeding pit, de-limbing, and de-hiding area.

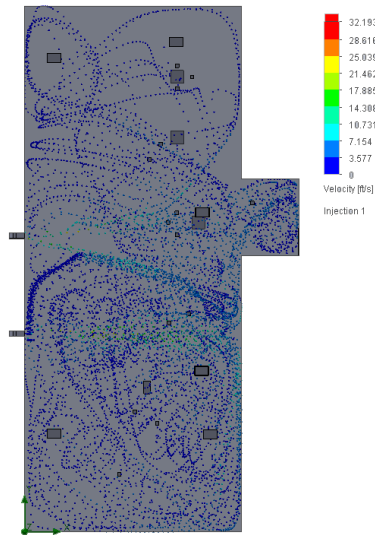


Figure 23: Skyview of Facility A when 20 particles are released from the entrance of the main hallway to the slaughter floor.

#### *IV.2.2 New Design*

A total of three new HVAC design were created for Facility A to create a more sanitary final product that would last longer on shelves and be safer for consumption. The first design is a displacement ventilation HVAC system. The second design is another displacement ventilation system with the same volumetric flow rate, but a lower intake velocity. The third design utilizes a hood. Here on out they will be labeled as Alpha, Beta, and Gamma, respectively. Alpha uses three intakes located at the rear of the facility, located five inches above the floor and evenly spaced. The velocity of air at the intakes is 3 ft/s in order to keep the intakes relatively small in size. The intakes measure 5 ft long and 3 ft tall. The large intake is needed to have a significant volumetric flow of 135 ft<sup>3</sup>/s. Six exhaust ports, measuring 3 ft long and 1 ft tall, are used to efficiently move air out of the facility. The three parallel exhaust ports at the front of the facility utilize an exhaust velocity of 4.7 ft/s and the three exhaust ports towards the middle of the facility have an

exhaust velocity of 10 ft/s. The offset of exhaust of velocity and position is used ensure most particles are exhausted at the very front of the facility and any particles that bypass them and begin to move to the rear of the facility will be captured by the second line of exhausts. The air exchange rate of 6.3 per hour is not high, but it is offset by the near unidirectional flow of air. The cool air moves across the slaughter floor, pushing most of the air towards the front of the facility (Figure 24). Vortices form at the front of the facility and some air streams return to the rear of the facility by traveling on both sides of the walls. Beta is nearly the same design as Alpha, however, the intakes are increased to 10 ft long and 4.5 ft tall to create an intake velocity of 1 ft/s. The air from the intakes is much more laminar across the facility than the Alpha design, and smaller vortices are formed (Figure 24). The decrease in turbulence significantly decreases any returning flow to the rear of the facility. The volumetric flow rate is the same as Alpha. The HVAC design in Gamma utilizes three intakes at the rear of the facility located 5 inches above the floor. The intakes measure 7 feet long and 2.5 feet tall ejecting air at 3 ft/s. Three exhaust ports, measuring 3 x 1 ft, are located at the front of the facility on the ceiling with a volumetric flow rate of 20.5 ft<sup>3</sup>/s each. The flanged hood is located 1 ft over the de-hiding zone with a 2.3 x 2.3 ft inlet and has a volumetric flow rate of 96 ft<sup>3</sup>/s. The volumetric flow rate  $Q$  was chosen using the equation for flanged hood efficiency using the vertical distance of the hood inlet from the contaminant site  $x$ , the area of the inlet  $A$ , and a capture velocity  $V$  equal to 500 ft/min.

$$Q = 0.75V(10x^2 + A)$$

The flow trajectory has more turbulence due to the high flow rate of the exhaust hood (Figure 24).

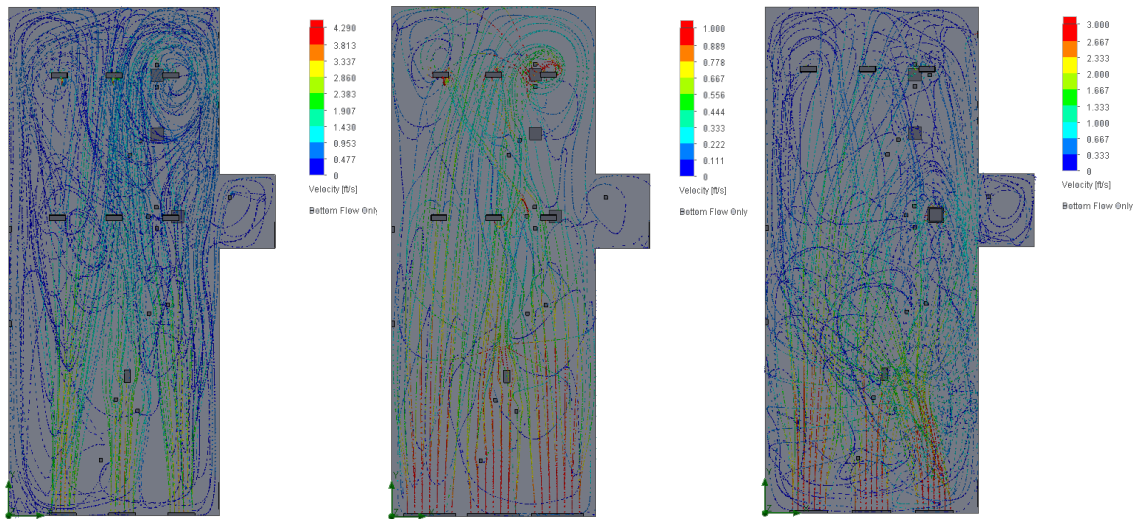


Figure 24: Skyview of the flow trajectories in the new design for Facility A. (Left) Skyview of the flow trajectories from the three intakes for the new Alpha HVAC design. (Middle) Skyview of the flow trajectories from the three intakes for the new Beta HVAC design. (Right) Skyview of the flow trajectories from the three intakes for the new Gamma HVAC design.

The heat from the workers, carcass, and 190 °F saw bath creates convection and raises the air currents towards the ceiling at the front of the facility. The inlet velocity of 3 ft/s in the Alpha design allows the primary flow to travel almost the length of the facility (Figure 25). However, the convection currents play a much bigger role in the Beta design where the outlet velocity is three times as slow (Figure 25). In the Gamma design, the primary flow splits into two early on due convection and the high volumetric flow rate of the hood (Figure 25). In all designs, the air that is capable of returning to the rear of the facility does not stay for long before returning back to the front.

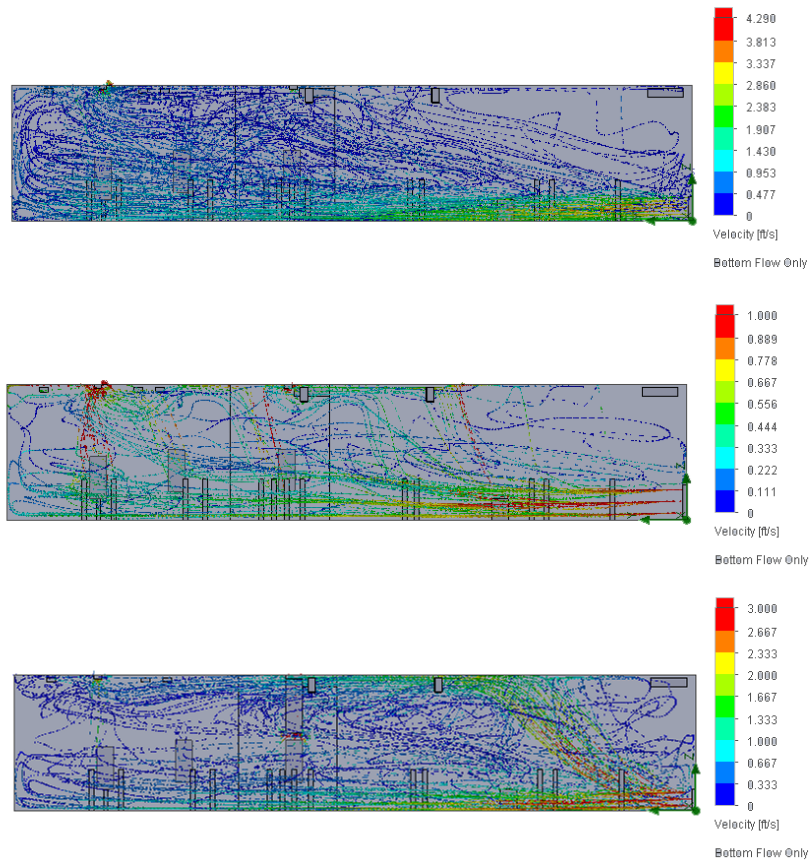
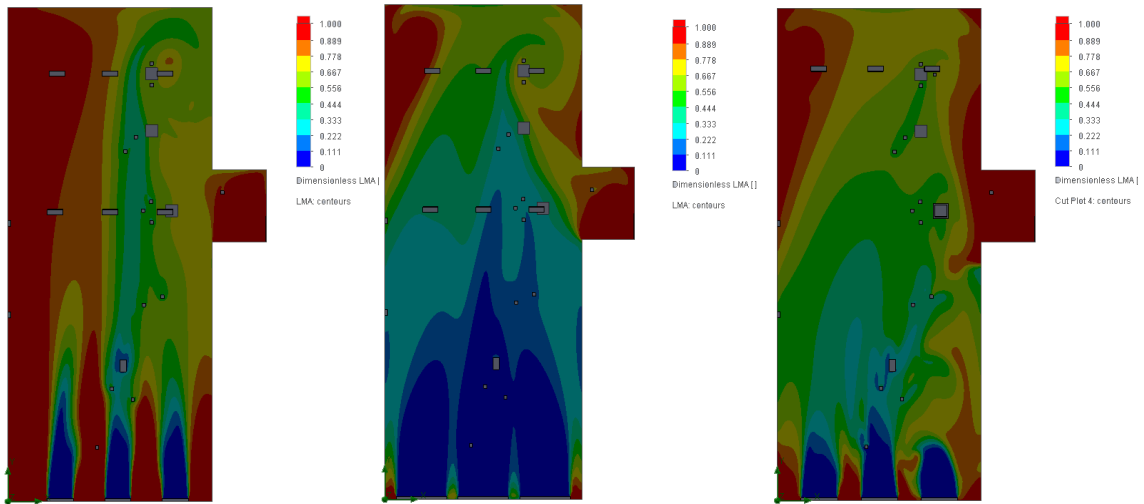


Figure 25: Side view of the flow trajectories for the new designs for Facility A. (Top) Side view of the flow trajectories from the three intakes for the new Alpha HVAC design. (Middle) Side view of the flow trajectories from the three intakes for the new Beta HVAC design. (Bottom) Side view of the flow trajectories from the three intakes for the new Gamma HVAC design.

The dimensionless LMA near ground level in design Alpha shows a significant portion of the left side of the facility to have low air movement (Figure 26 and 27). The larger intakes with slower velocity in design Beta are capable of forming a much better boundary movement of bulk air flow, and eliminates the most of the air returning alongside the walls (Figure 26 and 27). Design Gamma also maintains a formed front of air while near the ground, but the front breaks up around head level (Figure 26 and 27). In all cases, the line of workers causes faster air movement, especially in the vertical z-direction, causing faster

air movement around head level, consequently causing most of the air to rise at the front of the facility on the right side.



Figures 26: Skyview of the LMA near the floor in the new designs for Facility A. (Left) Skyview of the dimensionless LMA near ground level for the Alpha design. (Middle) Skyview of the dimensionless LMA near ground level for the Beta design. (Right) Skyview of the dimensionless LMA near ground level for the Gamma design.

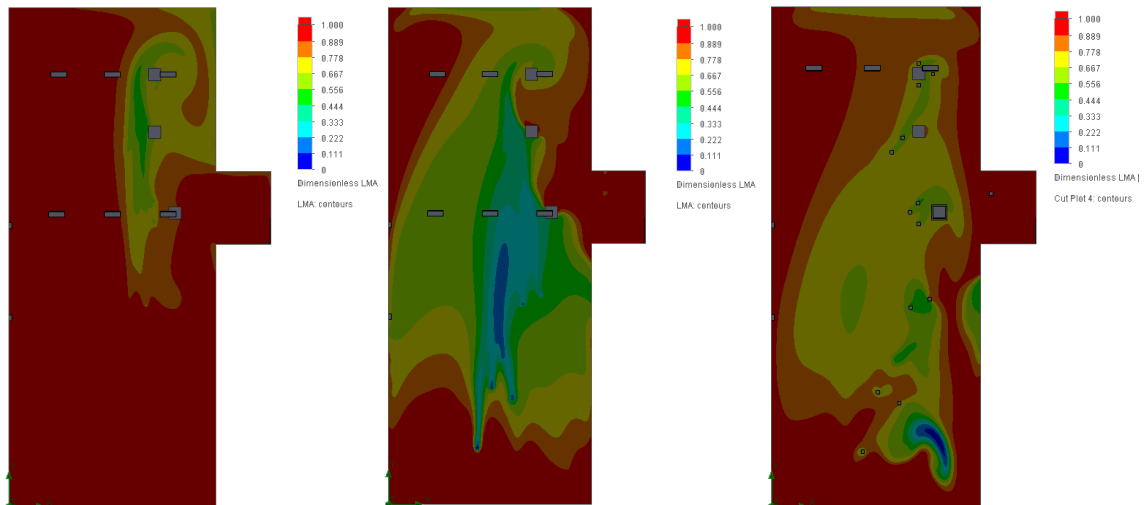


Figure 27: Skyview of the LMA at head level in the new designs for Facility A. (Left) Skyview of the dimensionless LMA at head level for the Alpha design. (Middle) Skyview of the dimensionless LMA at head level for the Beta design. (Right) Skyview of the dimensionless LMA at head level for the Gamma design.

Particle trace analysis was conducted in the same manner as for the old Facility design. 100 particles were released from the carcass in the bleeding pit for each design (Figure 28). Particles have a diameter of 1  $\mu\text{m}$ , there was no major difference between particles sized 1  $\mu\text{m}$  or 8  $\mu\text{m}$ . For the Alpha design, most of the particles are drawn through the exhausts at the front of the facility, while others are drawn through the secondary exhausts towards the middle of the facility. Six particles make the entire trip to the rear of the facility but are quickly moved back to the front. The CRE is 0.99, with only one particle not exiting through the exhaust within fifteen minutes. No particles reach the rear of the facility with the Beta design and the CRE is 1.00. The Gamma design has a CRE of 0.99 in fifteen minutes and one particle reaching the rear of the facility. The effects of convection on the particles in all designs may be seen in Figure 29.

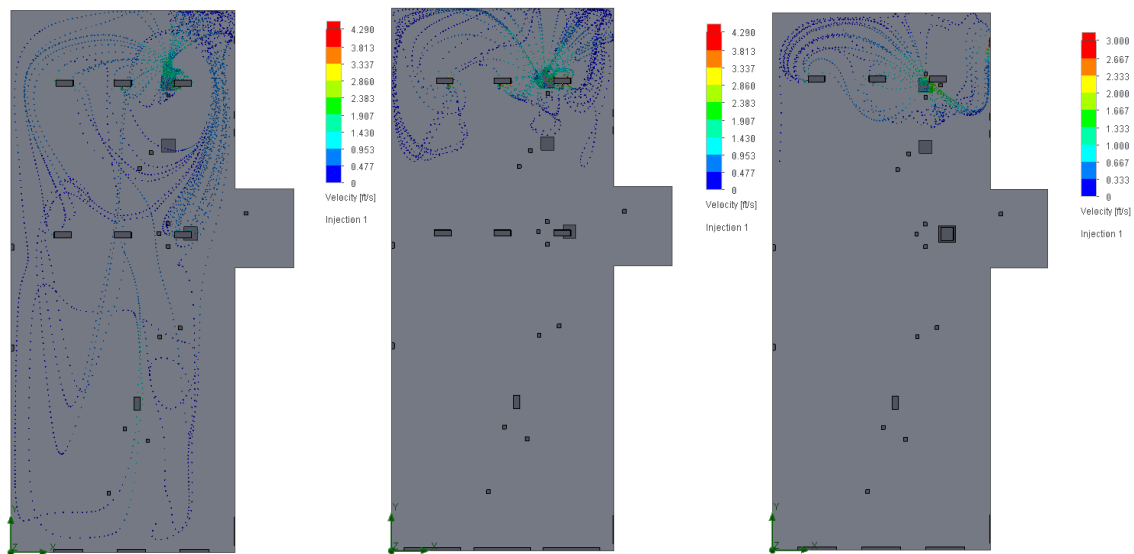


Figure 28: Skyview of particles released at the bleeding pit in the new designs of Facility A. (Left) Skyview of particle trace for 100 particles released from the bleeding pit in design Alpha. (Middle) Skyview of particle trace for 100 particles released from the bleeding pit in design Beta. (Right) Skyview of particle trace for 100 particles released from the bleeding pit in design Gamma.



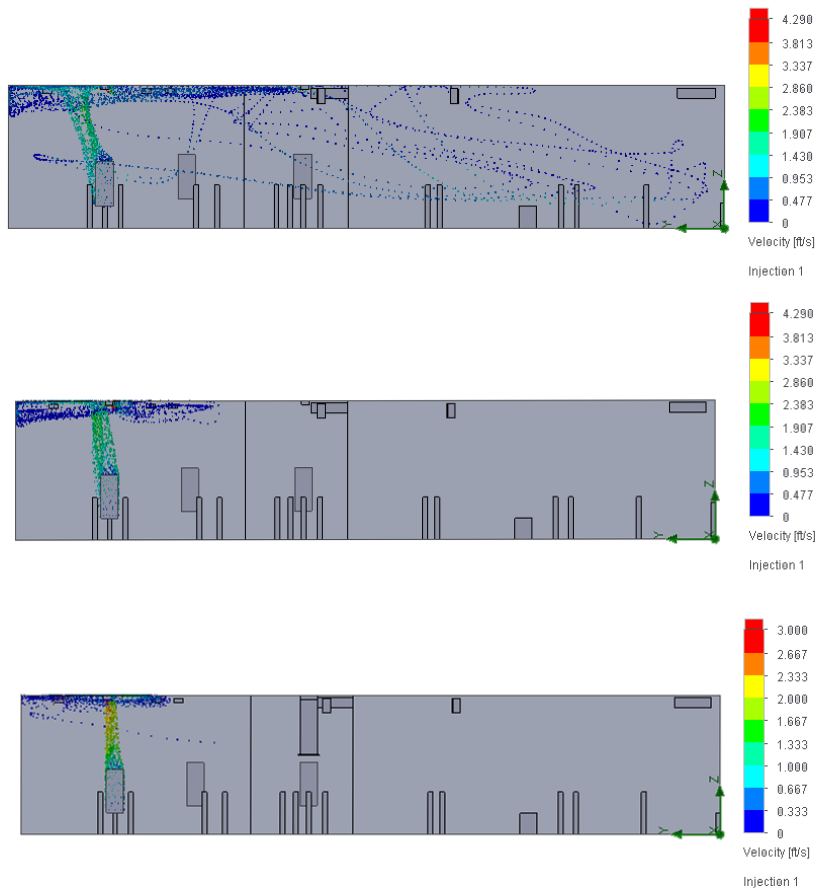


Figure 29: Side view of particles released at the bleeding pit in the new designs of Facility A. (Top) Side view of particle trace for 100 particles released from the bleeding pit in design Alpha. (Middle) Side view of particle trace for 100 particles released from the bleeding pit in design Bravo. (Bottom) Side view of particle trace for 100 particles released from the bleeding pit in design Gamma.

Next, 100 particles were released from both the carcass at the bleeding pit and the delimiting area for each design (Figure 30). At this stage, only a few more particles enter the rear of the facility in the Alpha design. The CRE is 0.975 for a fifteen minute run period. Particles that do reach the rear of the facility do not stay long and soon travel back to the front to be exhausted. The difference in all concentrations throughout the facility is noticeably different compared to the old design. No particles reach the rear of the facility in the Beta design and the CRE is 1.00. For the Gamma design, the hood catches most of

the particles coming from the de-limbing area, however three particles reach the rear of the facility. The CRE for this design is 0.98 for a fifteen minute run period.

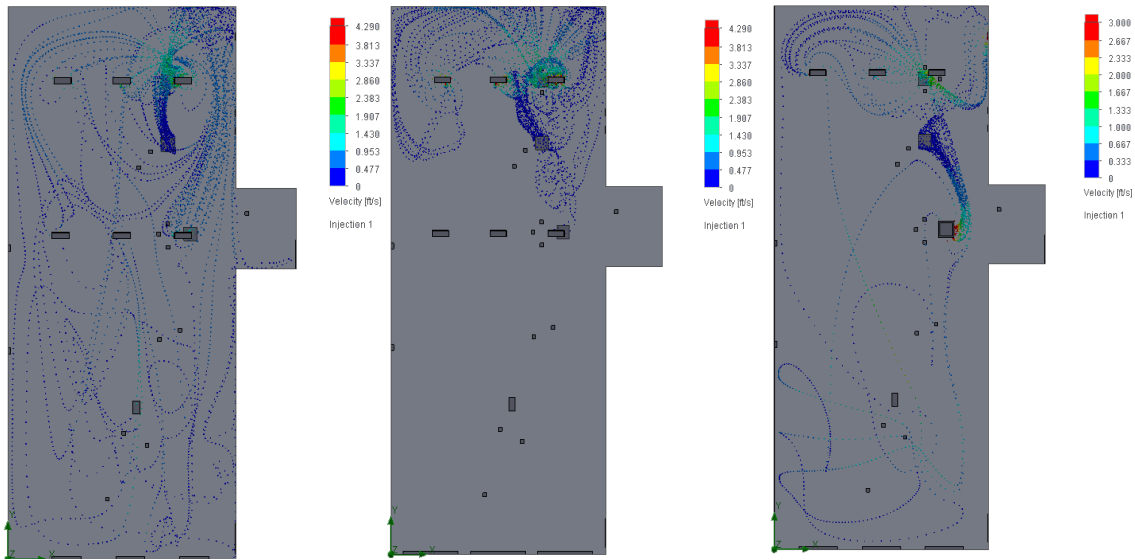


Figure 30: Skyview of particles released from the bleeding pit and de-limbing area in the new designs for Facility A. (Left) Skyview of 100 particles released from the bleeding pit and de-limbing area in design Alpha. (Middle) Skyview of 100 particles released from the bleeding pit and de-limbing area in design Beta. (Right) Skyview of 100 particles released from the bleeding pit and the de-limbing area in design Gamma.

Finally, 100 particles were released from the bleeding pit, de-limbing area, and the de-hiding area (Figure 31). In the Alpha design, the CRE is 0.98 for a fifteen-minute release period and 87% of particles remain in the unclean area. The Beta design allows a few less particles to reach the rear of the facility and also has a CRE of 0.98, but 96% of particles remain in the unclean area. The hood works the best of all when all three cattle are being processed in the Gamma design. 99.97% of particles remain in the unclean area and the CRE is 0.94 during a fifteen-minute release period.

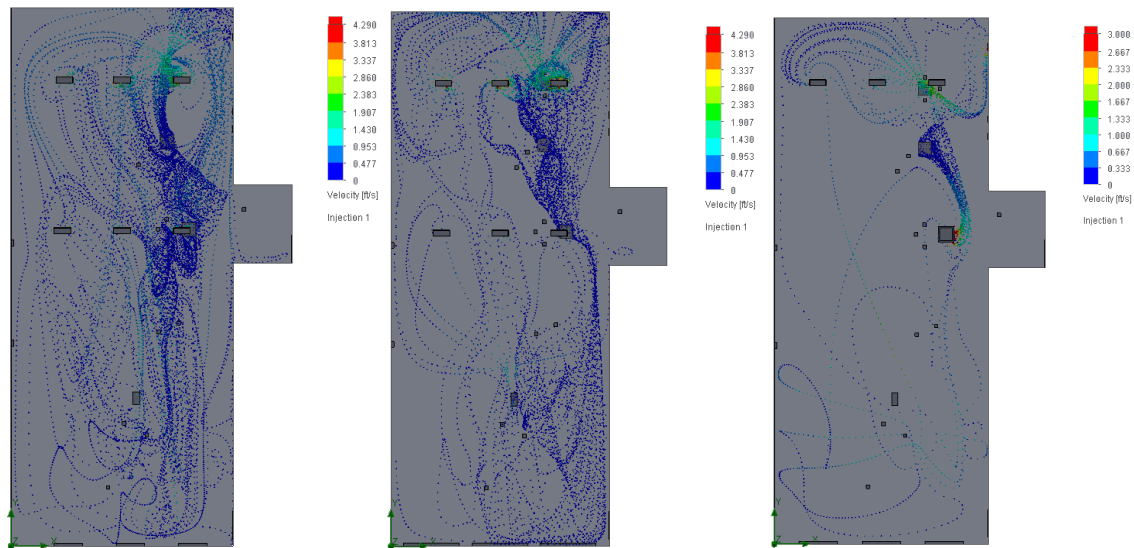


Figure 31: Skyview of particles released from the bleeding pit, de-limbing, and de-hiding area in the new designs of Facility A. (Left) Skyview of 100 particles released from the bleeding pit, de-limbing, and de-hiding area in design Alpha. (Middle) Skyview of 100 particles released from the bleeding pit, de-limbing area, and de-hiding area in design Beta. (Right) Skyview of 100 particles released from the bleeding pit, de-limbing area, and the de-hiding area in design Gamma.

As well, 20 particles were released from the area where a worker would enter the facility (Figure 32). The particles in the Alpha and Gama design are quickly drawn to the rear of the facility but are equally as quickly moved back towards the front. The Beta design does not allow the particles to reach the rear of the facility. Overall all these designs are much more efficient compared to the previous one. All requires less volumetric air flow and contain the bulk of bioaerosols to the front of the facility.

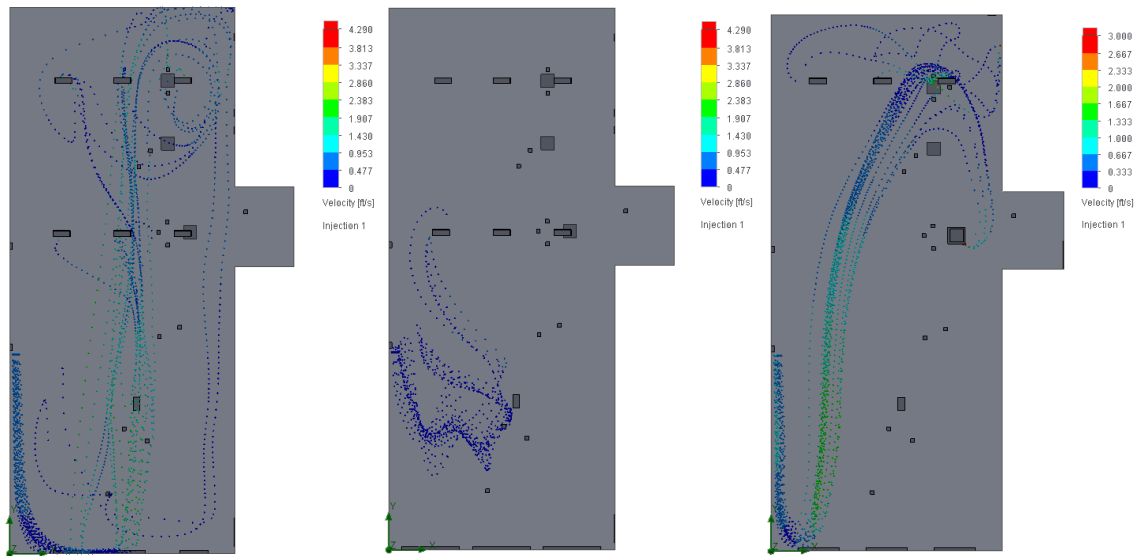


Figure 32: Skyview of particles released at the entrance of the new designs for Facility A. (Left) Skyview of 20 particles released from the entryway to the facility in the Alpha design. (Middle) Skyview of 20 particles released from the entryway to the facility in the Beta design. (Right) Skyview of 20 particles released from the entryway to the facility in the Gamma design.

### IV.3 Facility B qPCR Analysis

Testing at Facility B occurred during a one-day testing period in the morning. Therefore, the locations were only sampled once. Due to the limited space of the small facility, many of the processes occurred in the same place. For this same reason, only one continuous WWC was used, and was placed near the door to the freezer. The location of sampling for bleeding and de-limbing process was the same. As well, the sampling for the process of de-hiding and washing was in the same location. The only thing that changed was the time of sampling. Figure 33 displays the concentrations collected at each location in OTUs/m<sup>3</sup>. The largest concentration was collected near the freezer, with a concentration of log 5.8. The least amount of bioaerosols were collected during the washing phase, with a concentration of log 1.0. The total bacteria collected for the entire

morning session was log 5.8. This concentration was much higher than the morning average of log 4.46 collected at Facility A, and still higher than the average afternoon concentration of log 5.4. This is likely due to the very small slaughtering area in the rural Facility B and the fact that there was no intake or exhaust inside the slaughtering room. The only air movement was caused from an axial fan near the doorframe that pointed towards the carcass. The air only had one form of exit and that was the open door that led from the slaughter room to a hallway that was used for processing beef. It was decided that this location was of much importance for food safety, and a dynamic WWC was set up in the hallway and collected a TBC of log 3. It is very dangerous for the processing of the final meat product to be so close to the emission of bioaerosols and should be avoided at all costs. Furthermore, STEC *stx* was found inside the facility (Figure 33). The concentrations of STEC *stx* follow the same pattern as the TBC. *Salmonella* was only collected during the bleeding process with a concentration of log 6.6. More samples are needed for statistical analyses.

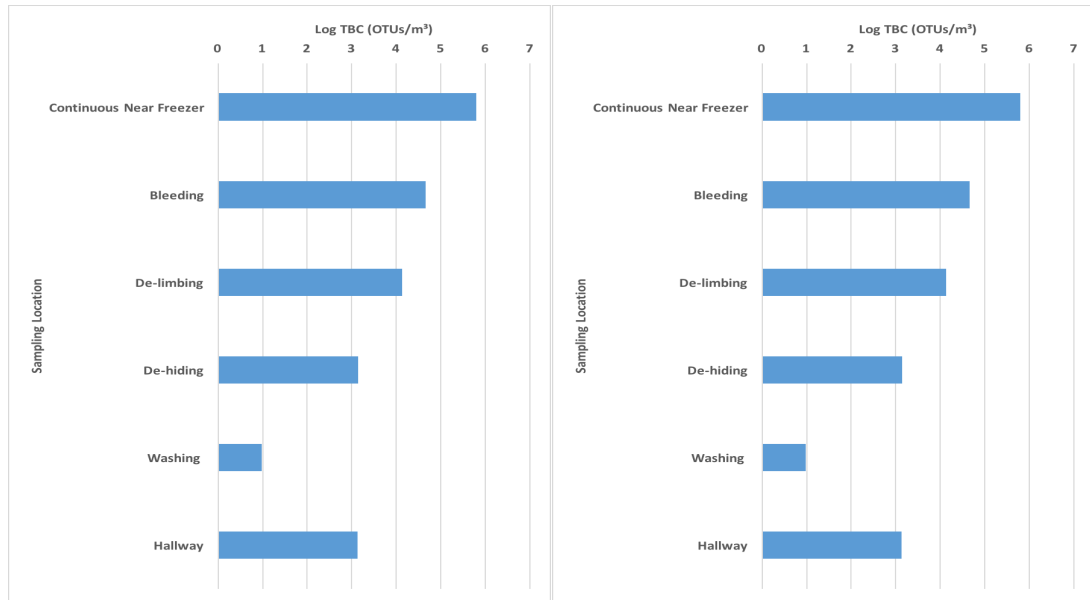


Figure 33: TBC and STEC collected at each location in Facility B. (Left) TBC collected at each sampling location at Facility B. (Right) Concentrations of STEC at each sampling location at Facility B.

## IV.4 Facility B CFD Analysis

### IV.4.1 Original Design

The air stream created from the singular fan in the slaughter room flows over both the de-hiding and bleeding location (Figure 34). When the air stream hits the opposite wall it is forced up towards the ceiling where it flows back towards the front of the room where it either re-enters the stream created from the fan or exits through the open door. The air stream flows dangerously around the entrance to the freezer, likely allowing bioaerosols to enter, and also exits through the door to the processing area (Figures 35-36). The LMA at collector level displayed in Figure 37 shows the area at the front of the facility near the door has slow air movement. The displacement of air from the fan is noticed wrapping around the facility. Two cattle were modeled as before in the two positions that were used

for the processing. The carcass was not hung from a hind leg as in Facility A, rather, the carcass was placed on a horizontal rack after the bleeding pit. Workers were modeled as before in Facility A, however, only two worked on the processing. The location of the continuous WWC collector near the freezer was in the area of fastest air movement compared to the other collectors. The dynamic WWC at the washing and de-hiding position was in the area of lowest air movement. The quickest air currents occur directly on or over the carcasses, likely causing many bacteria to become aerosolized. Temperature at head level in the modeled facility shows the heat emitted from the workers as well as the cow in the bleeding pit (Figure 37). The air is typically cooler around the edges of the facility where there is more air exchange.

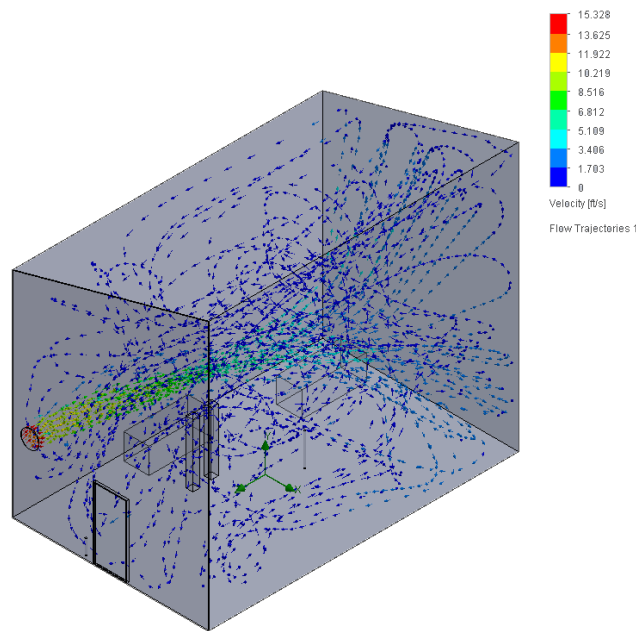


Figure 34: Isometric view of the flow trajectory inside of Facility B from the singular fan in the room. The only exit for air is through the open door.

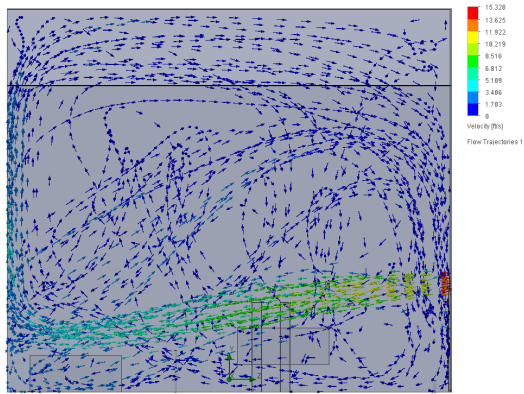


Figure 35: Side view of the flow trajectory inside of Facility B from the singular fan in the room.

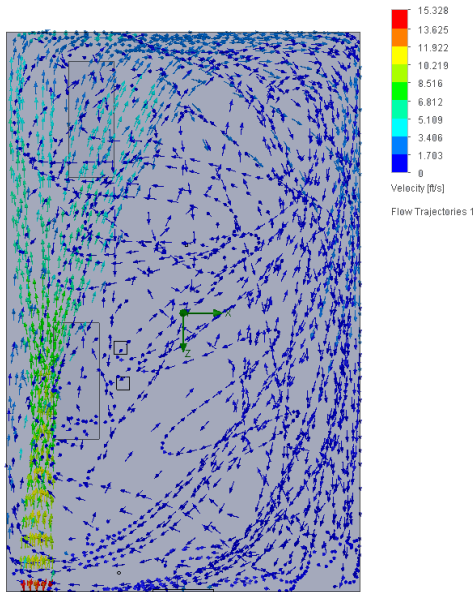


Figure 36: Skyview of the flow trajectory inside of Facility B from the singular fan in the room. Most of the flow wraps around the wall near the freezer and where the carcass hangs before entering the freezer.



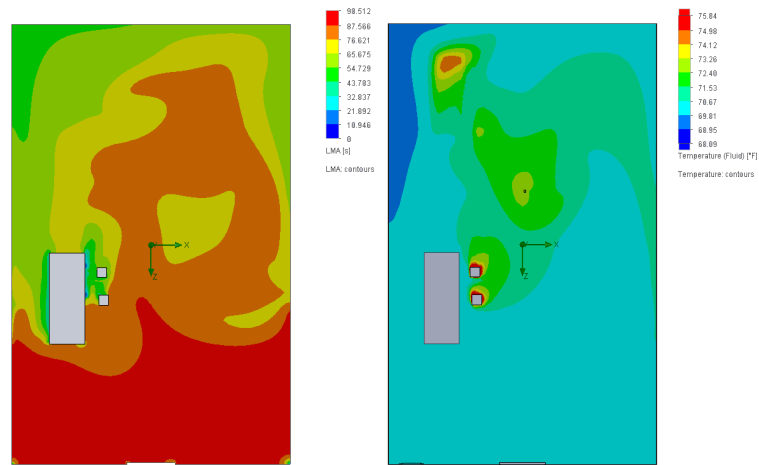


Figure 37: LMA and temperature in Facility B. (Left) LMA of Facility B at the WWC collector level. The air is most stagnant close to the door. (Right) Temperature at head level inside of Facility B. Heat generation from the carcass in the bleeding pit and the workers creates convection.

Velocity point profiles were taken from each location of the WWC to see if velocity and LMA had any effect on the concentrations collected. Since the collection location for the bleeding and de-limbing were the same, their TBC was averaged. The same was done for the de-hiding and washing TBC. It was found that as velocity increased, the concentration of collected bioaerosols also increased (Figure 38). In particular, the continuous WWC collector near the freezer had a very large concentration collected with a velocity magnitude of 1.37 ft/s. Although it had the largest velocity magnitude, the continuous WWC collector also had the largest negative velocity vector in the z-direction, which most likely aided significantly in the collector's capability of capture (Figure 38). As well, a large concentration of particles move over the continuous WWC's position because the fan blows the particles from the hide over to the collector. There was a significant correlation between increasing LMA and decreasing TBC (Figure 38).

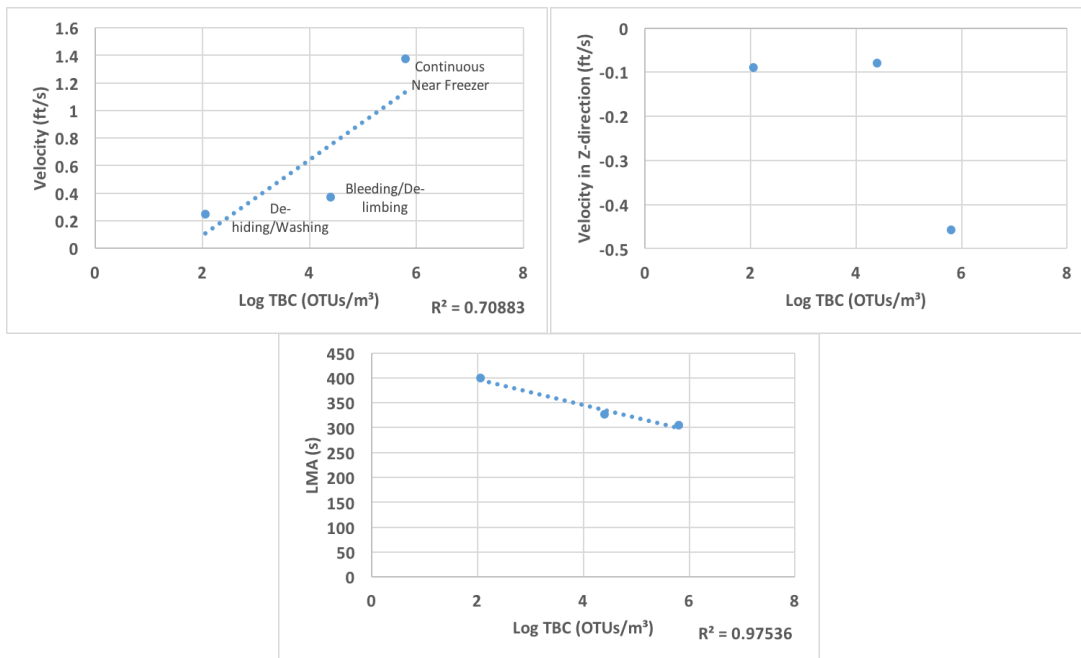


Figure 38: Velocity point profiles in Facility B. (Top Left) The velocity magnitude compared to the TBC in Facility B. As velocity increased, so did the concentration of bioaerosols collected. (Top Right) The velocity in the z-direction in Facility B compared to the TBC. The significantly larger negative velocity for the continuous WWC near the freezer likely aided the cyclone’s collection efficiency. (Bottom) The LMA compared to the TBC inside of Facility B. There is a strong trend with decreasing LMA, TBC increases.

Particle trace analysis was conducted to simulate bioaerosols emitting from the hide of the carcasses. A total of one hundred particles were first released from the carcass at the bleeding pit (Figure 39). Particles are immediately swept up by the flow created from the fan and hit the opposite wall where the particles are then lifted towards the ceiling, or to the opposite side where the freezer door is positioned. The only form of exit for the particles is through the door at the front of the slaughter room. Particle trace does not change significantly when particles are released from the de-hiding/washing position. The small space of this rural slaughter facility creates a lot of mixing. No major difference was seen between particles traces of  $1\ \mu\text{m}$  and  $8\ \mu\text{m}$ . However, the CRE value was lower for particles measuring  $8\ \mu\text{m}$ , just like Facility A. The CRE value does not tell us much

about the effectiveness of contaminant removal in this case because there are no exhaust ports, the open door is only acting like an exhaust port. The CRE value does give some information for the difference in latency period for particles of different sizes. It does appear that it is hard for the two tested facilities to effectively remove larger particles.

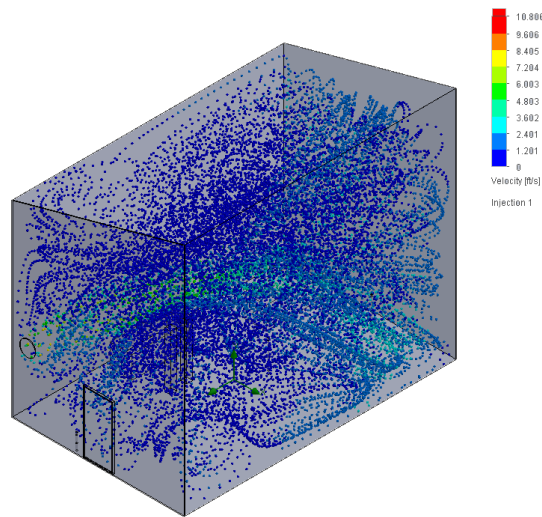


Figure 39: Particle trace of one hundred particles released from the carcass in the bleeding pit. The density of particle concentration is thick and spreads across the entire room. The only exit for the particles is through the door.

#### *IV.4.2 New Design*

A new HVAC was designed for Facility B to enhance its ability to remove particles and reduce particle movement in sensitive areas such as near the freezer, where the carcass hangs before entering the freezer, and out through the door into the hallway where meat is processed into a final product. There was a total of 2,515,981 cells used and a processing time of 12 hours. Due to the small size of the slaughter floor, and the heat generated from the carcass and the workers, a displacement ventilation system was used (Figures 40-41).

The dual intakes are placed five inches above the floor and emit cold air at 1 ft/s. The air stream spreads briefly across the floor before rising due to convection on the heat emitted by the workers and the carcass. A single exhaust port is located above the bleeding procedure to take advantage of the convection. Air is exhausted at 5 ft/s to create a negative air pressure inside the room. The negative pressure is needed in this case to stop the bioaerosols from traveling through the open door into the post-processing area of the facility (Figure 42). The airflow is also created such that the air rises above the carcass preparation so particles will not have a chance of landing before the carcass enters the chiller (Figure 43). The dimensionless LMA near the floor and at head level (Figure 44) displays the movement of air through the intakes and the door. As the air rises, the air on the right side becomes slow and latent while the air over the workers and carcasses rises quickly towards the exhaust and ceiling.

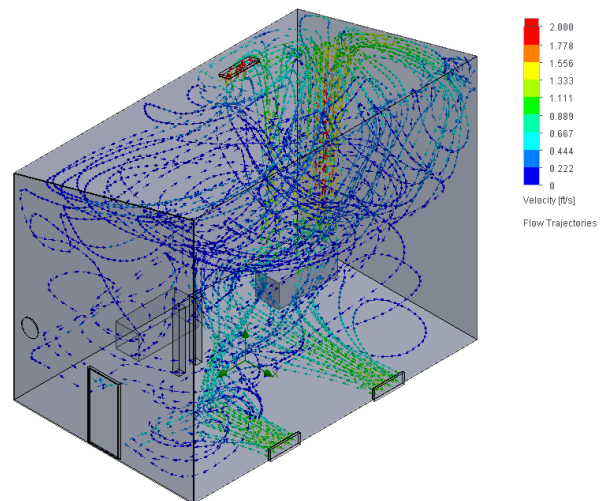


Figure 40: The flow trajectory in isometric view of the new displacement ventilation system for Facility B. Slow, 1 ft/s velocity flow through the intakes prevents harsh mixing of the air.

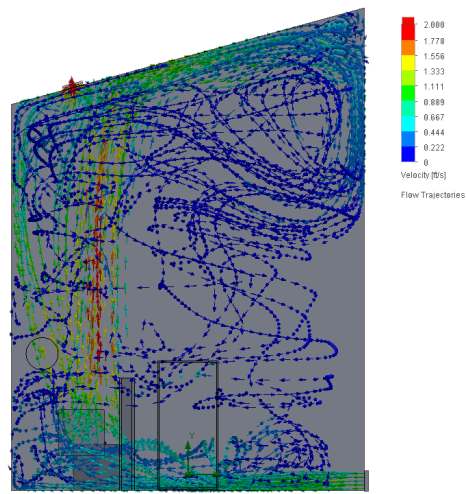


Figure 41: Front view of the new HVAC design for facility B. The flow trajectory of air rises upon meeting with the workers and the carcass at the bleeding pit due to convection.

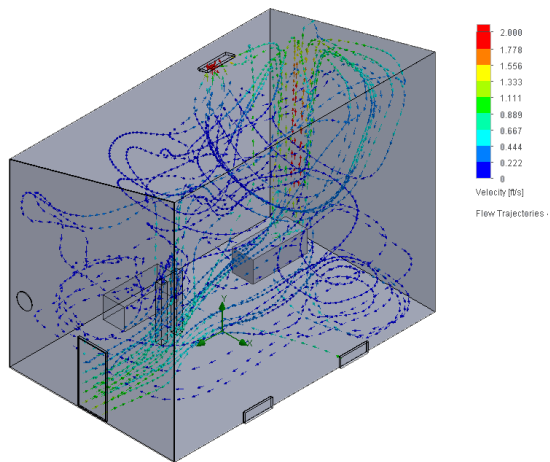


Figure 42: Isometric view of the flow trajectory coming from the open door. The exhaust causes negative pressure in the room, causing air to flow into the slaughter room from the door, preventing bioaerosols from entering the post-processing area.

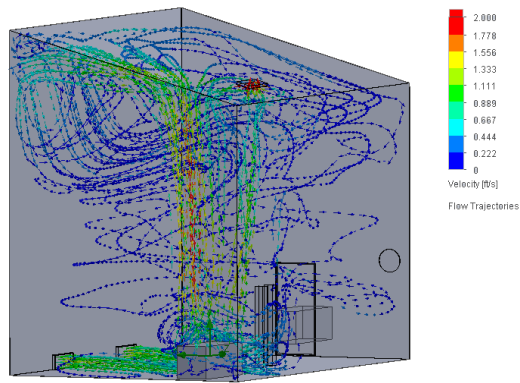


Figure 43: View of the rear of the facility looking where the freezer door is located. There is limited flow trajectories in the area of the freezer.

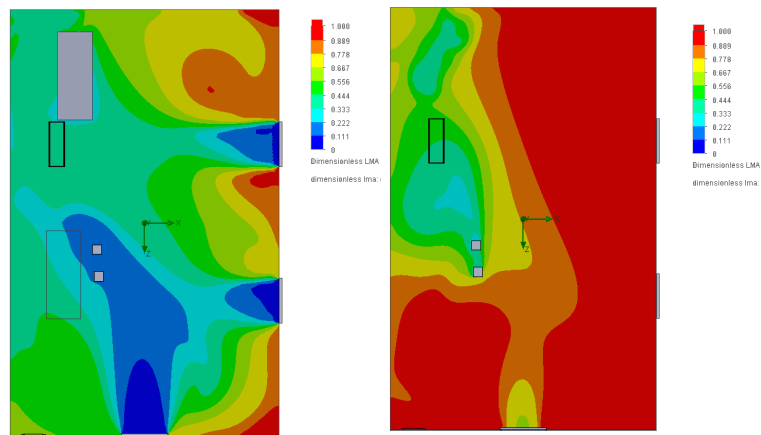
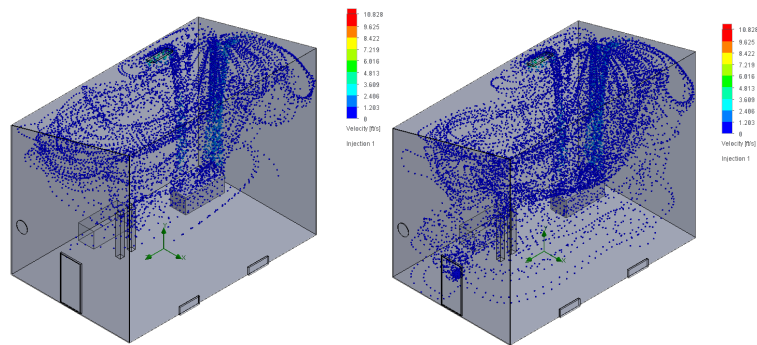


Figure 44: LMA in the new design of Facility B. (Left) The dimensionless LMA at near floor level. Small vortices form near the wall of the freezer. Air flow can be seen from the door and the two inlets. (Right) The dimensionless LMA at head level. The air on the right face of the wall where the carcass hangs before entering the chiller is latent, while the airflow created from convection becomes the cause for the fastest movement of air in the room.

Particle trace analysis from the bleeding area with  $1\ \mu\text{m}$  diameters (Figures 45 and 46) displays the particles rising immediately to the ceiling. Only a few particles cross near the freezer door. The CRE for this system is 0.86. When particles are changed to  $8\ \mu\text{m}$  (Figures 45 and 46) the system is less efficient, with a CRE of 0.80. The noticeable difference is the amount of particles that have drifted to a lower height. When particles are

released from the de-hiding area, the latent air flow near the door becomes a problem. Small vortices there harbor any particles that have entered the area. The problem is not solved with increasing exhaust speed, inlet location, or by creating a secondary exhaust over the area. A total of 10 particles out of 100 settled in this region. Knowing the location of the problem, it could be solved by either putting a heat source in the region, or by placing a WWC collector in the region to catch the descending particles. The displacement ventilation system would not cost much due to its low intake and exhaust flow rate. The negative air pressure that the system creates stops the majority of bioaerosols from traveling through the open door into the rest of the processing facility.



Figures 45: Isometric views of particle traces in the new design of Facility B. (Left) Isometric view of Facility B observing 100 particles with a diameter of 1  $\mu\text{m}$  emitted from the carcass in the bleeding pit. (Right) Isometric view of Facility B observing 100 particles with a diameter of 8  $\mu\text{m}$  emitted from the carcass in the bleeding pit.

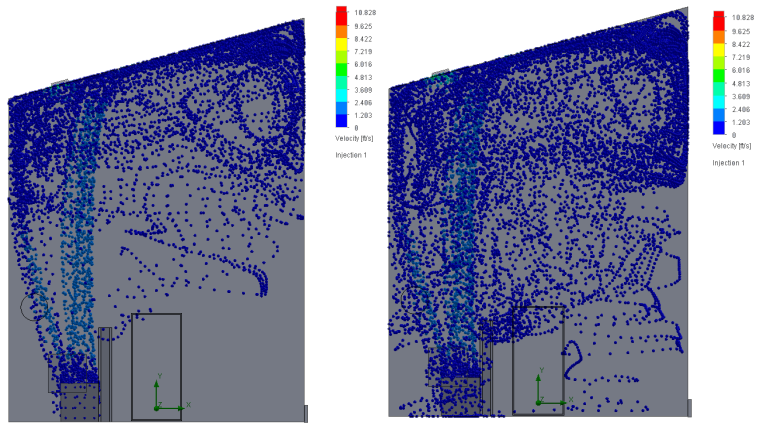


Figure 46: Front view of particles traces in the new design for Facility B. (Left) Front view of Facility B observing 100 particles emitted from the carcass in the bleeding pit. The particles rise due to convection and stay at a safe height. (Right) Front view of Facility B observing the particles that become caught in vortices in the lower left side of the facility.



## CHAPTER V

### CONCLUSIONS

In part, the purpose of this study was to enumerate the total concentrations of bioaerosols, as well as STEC and *Salmonella*, in two different beef slaughter facilities. As well, CFD was utilized to analyze the flow patterns and track aerosolized particles. Using WWC collectors, the results displayed that the concentrations of bioaerosols collected is not only dependent on the location of the physical procedures of processing the carcasses, but is also highly dependent on the movement of air in the facility. STEC and *Salmonella* were found aerosolized inside of Facility A. Contrary to many studies, a dynamic WWC unit placed near the de-hiding area in Facility A collected the least amount of bioaerosols. However, the continuous WWC placed on the opposite side of the de-hiding area collected the second highest concentration of bioaerosols and was significantly different. Upon inspection of the flow trajectories, it was apparent that the dynamic WWC was “upstream” of the airflow that was directed towards the de-hiding area, while the continuous WWC unit was downstream of the flow, and was subsequently able to collect all the particles that were becoming aerosolized. The general trend showed that bioaerosol counts, specifically *Salmonella* and STEC *eae*, increased in Facility A with each passing day, displaying the inability of the facility to effectively remove particles during processing. As well, no significant correlation was found between the concentration of bioaerosols and the number of workers or the distance of the collectors from the carcasses. Furthermore, the concentrations of TBC and STEC *stx* significantly increased between the

morning and afternoon phases of processing. The highest concentration of bioaerosols in Facility A were collected at the de-limbing area, which also had the highest LMA. However, only the bleeding pit was significantly different from the de-limbing, near freezer, and the de-hiding area. This could be due to its position at the very front of the facility. Further analysis with Illumina Sequencing needs to be performed to verify the quantity of bacteria found from qPCR. Temperature and humidity data was collected during testing at Facility A, but no significant relationship was found for TBC. However, the trend did describe increasing temperature with increasing TBC. The temperatures near the freezer were significantly higher than the temperatures measured near the de-hider and the outside temperature seemed to have an effect on the temperature and humidity inside the facility.

Using velocity point profiles at the inlet location of the WWC in the CFD model of Facility A, it was also noticed that the dynamic WWC in the de-limbing area had the largest negative velocity in the z-direction, or vertical direction. This likely aided the collector greatly in its ability to capture bioaerosols. This correlates with the continuous WWC near the freezer, which captured the highest concentration collected at Facility B and also had the largest negative velocity in the z-direction compared to the other collectors. Facility B was found to have a correlation between decreasing LMA and increasing TBC collected. The CFD model showed that these areas of higher velocity still had higher particle density.

Particle trace analysis in Facility A emitted particles from three significant locations in the beef slaughter process and allowed CRE values of the HVAC systems to be

determined throughout a typical day and track the movement of bioaerosols. Facility A was found to have an enormous spread of bioaerosols across the entire floor and near the freezer door. This type of bioaerosol dispersion can be especially dangerous for consumers. The intake closer to the front of the facility was found to eject air directly on the de-hiding area and loose vortices formed at the front and rear of the facility. Bioaerosols emitted from workers entering from the main hallway into the slaughter floor were found to spread throughout the facility. CRE decreased in both facilities when 8  $\mu\text{m}$  particles simulating an agglomeration were used compared to particles measuring 1  $\mu\text{m}$ . This shows that a serious revision is needed for beef slaughter facilities to enhance sanitation and limit the spread of bioaerosols to the clean areas of their facilities. The only outlet in the Facility B slaughter floor was the doorway leading to the post-processing portion of the facility that prepared meats for customers. All particles eventually exited this way. This could easily allow bioaerosols to adhere to the finished meat product, and the airflow constraints in rural beef slaughter facilities needs to be changed. The lack of any ventilation in Facility B caused the WWC to collect a higher TBC during the single morning session than any of the other morning sessions at Facility A.

New HVAC systems were designed for both facilities to limit the spread of bioaerosols. For both facilities, displacement ventilation was the best at reducing particle spread. Piston flow did not work at Facility A due to the convection caused by cattle, workers, and equipment. The CRE in Facility A was improved to 0.975 and above, and limited particle movement to the rear of the facility drastically. No change was found in the CRE when particle size was increased to 8  $\mu\text{m}$ . However, the CRE changed from 0.86

to 0.80 when particle size was increased. The new design in Facility B reduces particles exiting the door into the hallway by utilizing a negative pressure gradient, causing air to flow from the door into the slaughter room. Both methods have a low volumetric flow rate and will not require much energy.

Further studies should incorporate larger sample sizes with more facilities, specifically large facilities with a high cattle throughput. Air sampling can take up large portions of the day and needs to be planned carefully. It would be wise to receive the blueprints of beef facilities first and model the HVAC airflow. Then, upon inspection of the modeled flow, specific points of interest can be chosen for collection inside the facility. Temperature and humidity data should be taken at every collection site as well as outside of the facility. Furthermore, it would be beneficial to take bioaerosol samples at the exhaust of the beef facilities. DNA should be sent for Illumina Sequencing so the microbiomes can be analyzed between collection sites in the facilities, between feedlots and facilities, and to verify the qPCR data. As well, the UAS collector needs further testing to discover its efficiency in collection of bioaerosols. HVAC systems can be further optimized with respect to energy usage, however the new designs presented in Facility A require less flow rate than the original design

Through the use of high volume, efficient bioaerosol collectors, concentrations of bacteria and pathogens were enumerated. The cyclone collectors reduce stress to bioaerosols and concentrate the effluent, allowing for large collection concentrations of bioaerosols. The use of DNA analysis instead of traditional plating techniques allowed not just viable but also non-viable bioaerosol concentrations to be found. Using blueprints

of the facilities, models were created and the CFD analysis correlated well with the experimental collection results. This is the first time bioaerosol concentrations have been used in tandem with CFD to track and verify particles in beef slaughterhouses. The results display a giant need to redesign the HVAC systems in these types of facilities. Recommendations for redesign have been proposed. The proposed designs were modeled, tested, and found to significantly increase plant sanitation.

## REFERENCES

1. Mor-Mur, M. and J. Yuste, *Emerging Bacterial Pathogens in Meat and Poultry: An Overview*. Food and Bioprocess Technology, 2009. **3**(1): p. 24.
2. Su, L.H. and C.H. Chiu, *Salmonella: clinical importance and evolution of nomenclature*. Chang Gung Med J, 2007. **30**(3): p. 210-9.
3. Center for Disease Control and Prevention. *Escherichia Coli*. January 6, 2017]; Available from: <https://www.cdc.gov/ecoli/general/index.html>.
4. Scharff, R.L., *Economic burden from health losses due to foodborne illness in the United States*. J Food Prot, 2012. **75**(1): p. 123-31.
5. Hinds, W.C., *Aerosol technology : properties, behavior, and measurement of airborne particles*. 1982, New York: J. Wiley. xix, 424 p.
6. Stokes, G.G., *On the effect of the internal friction of fluids on the motion of pendulums*. Cambridge Philosophical Society Transactions. 1851, Cambridge: Pitt Press. 99 p.
7. Cunningham, E., *On the Velocity of Steady Fall of Spherical Particles through Fluid Medium*. Proceedings of the Royal Society of London. Series A, 1910. **83**(563): p. 357-365.
8. Donaldson, K., et al., *Combustion-derived nanoparticles: a review of their toxicology following inhalation exposure*. Part Fibre Toxicol, 2005. **2**: p. 10.
9. Ogden, L.E., *Life in the Clouds*. BioScience, 2014. **64**(10): p. 861-867.
10. Mainelis, G., *Collection of Airborne Microorganisms by Electrostatic Precipitation*. Aerosol Science and Technology, 1999. **30**(2): p. 127-144.
11. Mainelis, G., et al., *Electrical charges on airborne microorganisms*. Journal of Aerosol Science, 2001. **32**(9): p. 1087-1110.
12. Park, J.-W., et al., *Fast Monitoring of Indoor Bioaerosol Concentrations with ATP Bioluminescence Assay Using an Electrostatic Rod-Type Sampler*. PLoS ONE, 2015. **10**(5): p. e0125251.
13. Kreider, J.F., *Handbook of heating, ventilation, and air conditioning*. Mechanical engineering handbook series. CRC Press. 2000.

14. Yu, B.F., et al., *Review of research on air-conditioning systems and indoor air quality control for human health*. International Journal of Refrigeration, 2009. **32**(1): p. 3-20.
15. Cecchini, C., et al., *Effects of antimicrobial treatment on fiberglass-acrylic filters*. J Appl Microbiol, 2004. **97**(2): p. 371-7.
16. al., C.e., *Ventilation, Good Indoor Air Quality and Rational Use of Energy*. 2003. **Report No 23**(Urban Air, Indoor Environment and Human Exposure).
17. A.M. van Buren, J.A.M., H.M.J. van Eijk, J. O'Brien, S.D. Pannell, D. Lawrence, R. Hopman, W.G.J.M. van Tongeren, *The prevention and control of Legionella spp. (including Legionnaires' disease) in food factories*. Trends in Food Science & Technology, 2002. **13**: p. 380-384.
18. Byrne, B., et al., *An assessment of the microbial quality of the air within a pork processing plant*. Food Control, 2008. **19**(9): p. 915-920.
19. Prendergast, D.M., et al., *The effect of abattoir design on aerial contamination levels and the relationship between aerial and carcass contamination levels in two Irish beef abattoirs*. Food Microbiology, 2004. **21**(5): p. 589-596.
20. Buncic, S. and J. Sofos, *Interventions to control Salmonella contamination during poultry, cattle and pig slaughter*. Food Research International, 2012. **45**(2): p. 641-655.
21. Richardson, L.F., *The Approximate Arithmetical Solution by Finite Differences of Physical Problems Involving Differential Equations, with an Application to the Stresses in a Masonry Dam*. Philosophical Transactions of the Royal Society of London. Series A, Containing Papers of a Mathematical or Physical Character, 1911. **210**(459-470): p. 307-357.
22. Burfoot, D., et al., *Fogging for the disinfection of food processing factories and equipment*. Trends in Food Science & Technology, 1999. **10**(6-7): p. 205-210.
23. Rouaud, O. and M. Havet, *Numerical investigation on the efficiency of transient contaminant removal from a food processing clean room using ventilation effectiveness concepts*. Journal of Food Engineering, 2005. **68**(2): p. 163-174.
24. Driss, Z., et al., *Numerical simulation and experimental validation of the turbulent flow around a small incurved Savonius wind rotor*. Energy, 2014. **74**: p. 506-517.
25. Chen Q, M.A., *Simulation of a multiple-nozzle diffuser*. 1991. **12th AIVC Conference**: p. 24-27.

26. Jericho, K.W., J. Ho, and G.C. Kozub, *Aerobiology of a high-line speed cattle abattoir*. J Food Prot, 2000. **63**(11): p. 1523-8.
27. Okraszewska-Lasica, W., et al., *Airborne Salmonella and Listeria associated with Irish commercial beef, sheep and pig plants*. Meat Science, 2014. **97**(2): p. 255-261.
28. Pearce, R.A., J.J. Sheridan, and D.J. Bolton, *Distribution of airborne microorganisms in commercial pork slaughter processes*. Int J Food Microbiol, 2006. **107**(2): p. 186-91.
29. Marjatta Rahkio, T. and H.J. Korkeala, *Airborne Bacteria and Carcass Contamination in Slaughterhouses*. Journal of Food Protection, 1997. **60**(1): p. 38-42.
30. Heldman, D.R., *Factors Influencing Air-borne contamination of foods. A review*. Journal of Food Science, 1974. **39**(5): p. 962-969.
31. Lighthart, B., A.J. Mohr, and SpringerLink (Online service), *Atmospheric Microbial Aerosols Theory and Applications*. 1994, Springer US,: Boston, MA. p. 1 online resource.
32. Beach, J.C., E.A. Murano, and G.R. Acuff, *Prevalence of Salmonella and Campylobacter in beef cattle from transport to slaughter*. J Food Prot, 2002. **65**(11): p. 1687-93.
33. Van Donkersgoed, J., T. Graham, and V. Gannon, *The prevalence of verotoxins, Escherichia coli O157:H7, and Salmonella in the feces and rumen of cattle at processing*. Can Vet J, 1999. **40**(5): p. 332-8.
34. Davies, P.R., et al., *Prevalence of Salmonella in finishing swine raised in different production systems in North Carolina, USA*. Epidemiology and Infection, 1997. **119**(2): p. 237-244.
35. Proux, K., et al., *Contamination of pigs by nose-to-nose contact or airborne transmission of Salmonella Typhimurium*. Vet Res, 2001. **32**(6): p. 591-600.
36. Schmidt, J.W., et al., *Detection of Escherichia coli O157:H7 and Salmonella enterica in air and droplets at three U.S. commercial beef processing plants*. J Food Prot, 2012. **75**(12): p. 2213-8.
37. Kotula, A.W. and J.A. Kinner, *Airborne Microorganisms in Broiler Processing Plants*. Appl Microbiol, 1964. **12**: p. 179-84.



38. Cvjetanovic, B., *Determination of bacterial air pollution in various premises*. J Hyg (Lond), 1958. **56**(2): p. 163-8.
39. Sofos, J.N., et al., *Sources and extent of microbiological contamination of beef carcasses in seven United States slaughtering plants*. J Food Prot, 1999. **62**(2): p. 140-5.
40. Errington, F.P. and E.O. Powell, *A cyclone separator for aerosol sampling in the field*. J Hyg (Lond), 1969. **67**(3): p. 387-99.
41. Lin, W.-H. and C.-S. Li, *The Effect of Sampling Time and Flow Rates on the Bioefficiency of Three Fungal Spore Sampling Methods*. Aerosol Science and Technology, 1998. **28**(6): p. 511-522.
42. Jensen, P.A., et al., *Evaluation of eight bioaerosol samplers challenged with aerosols of free bacteria*. Am Ind Hyg Assoc J, 1992. **53**(10): p. 660-7.
43. Chopyk, J., et al., *Presence of pathogenic Escherichia coli is correlated with bacterial community diversity and composition on pre-harvest cattle hides*. Microbiome, 2016. **4**(1): p. 9.
44. Lundbeck, H., U. Plazikowski, and L. Silverstolpe, *The Swedish Salmonella outbreak of 1953*. Journal of Applied Bacteriology, 1955. **18**(3): p. 535-548.
45. Melling, J., et al., *Identification of a novel enterotoxigenic activity associated with Bacillus cereus*. Journal of Clinical Pathology, 1976. **29**(10): p. 938-940.
46. Borch, E. and P. Arinder, *Bacteriological safety issues in red meat and ready-to-eat meat products, as well as control measures*. Meat Science, 2002. **62**(3): p. 381-390.
47. Borch, E., M.-L. Kant-Muermans, and Y. Blixt, *Bacterial spoilage of meat and cured meat products*. International Journal of Food Microbiology, 1996. **33**(1): p. 103-120.
48. Scallan, E., et al., *Foodborne Illness Acquired in the United States—Major Pathogens*. Emerging Infect Dis, 2011. **17**(1): p. 7-15.
49. Elaine, S., et al., *Foodborne Illness Acquired in the United States—Unspecified Agents*. Emerging Infect Dis, 2011. **17**(1): p. 16.
50. Riley, L.W., et al., *Hemorrhagic Colitis Associated with a Rare Escherichia coli Serotype*. New England Journal of Medicine, 1983. **308**(12): p. 681-685.

51. Griffin, P.M. and R.V. Tauxe, *The Epidemiology of Infections Caused by Escherichia coli O157: H7, Other Enterohemorrhagic E. coli, and the Associated Hemolytic Uremic Syndrome*. *Epidemiologic Reviews*, 1991. **13**(1): p. 60-98.
52. Johannes, L. and W. Romer, *Shiga toxins [mdash] from cell biology to biomedical applications*. *Nat Rev Micro*, 2010. **8**(2): p. 105-116.
53. Sandvig, K., et al., *Pathways followed by ricin and Shiga toxin into cells*. *Histochemistry and Cell Biology*, 2002. **117**(2): p. 131-141.
54. Welinder-Olsson, C. and B. Kaijser, *Enterohemorrhagic Escherichia coli (EHEC)*. *Scandinavian Journal of Infectious Diseases*, 2005. **37**(6-7): p. 405-416.
55. Rangel, J.M., et al., *Epidemiology of Escherichia coli O157: H7 outbreaks, United States, 1982–2002*. *Emerg Infect Dis*, 2005. **11**.
56. Breuer, T., et al., *A multistate outbreak of Escherichia coli O157:H7 infections linked to alfalfa sprouts grown from contaminated seeds*. *Emerging Infect Dis*, 2001. **7**(6): p. 977-982.
57. Bitton, G., *Encyclopedia of Environmental Microbiology: Sp-Z; Index*. 2002: Wiley.
58. *An Introduction to Next-Generation Sequencing Technology*. Illumina Inc. 2016.
59. McFarland, A.R., et al., *Wetted Wall Cyclones for Bioaerosol Sampling*. *Aerosol Science and Technology*, 2010. **44**(4): p. 241-252.
60. King, M.D. and A.R. McFarland, *Bioaerosol Sampling with a Wetted Wall Cyclone: Cell Culturability and DNA Integrity of Escherichia coli Bacteria*. *Aerosol Science and Technology*, 2012. **46**(1): p. 82-93.
61. Rahn, K., et al., *Amplification of an invA gene sequence of Salmonella typhimurium by polymerase chain reaction as a specific method of detection of Salmonella*. *Mol Cell Probes*, 1992. **6**(4): p. 271-9.
62. Bassler, H.A., et al., *Use of a fluorogenic probe in a PCR-based assay for the detection of Listeria monocytogenes*. *Applied and Environmental Microbiology*, 1995. **61**(10): p. 3724-3728.
63. Nayak, R., T.M. Stewart, and M.S. Nawaz, *PCR identification of Campylobacter coli and Campylobacter jejuni by partial sequencing of virulence genes*. *Mol Cell Probes*, 2005. **19**(3): p. 187-93.

64. Clarridge, J.E., *Impact of 16S rRNA gene sequence analysis for identification of bacteria on clinical microbiology and infectious diseases*. Clinical microbiology reviews, 2004. **17**(4): p. 840-862.
65. Possé, B., et al., *Metabolic and genetic profiling of clinical O157 and non-O157 Shiga-toxin-producing Escherichia coli*. Research in Microbiology, 2007. **158**(7): p. 591-599.
66. VanGuilder, H.D., K.E. Vrana, and W.M. Freeman, *Twenty-five years of quantitative PCR for gene expression analysis*. Biotechniques, 2008. **44**(5): p. 619.
67. Tong, Y. and B. Lighthart, *The Annual Bacterial Particle Concentration and Size Distribution in the Ambient Atmosphere in a Rural Area of the Willamette Valley, Oregon*. Aerosol Science and Technology, 2000. **32**(5): p. 393-403.
68. Frankel, M., et al., *Seasonal variation of indoor microbial exposures and their relations to temperature, relative humidity and air exchange rates*. Applied and Environmental Microbiology, 2012: p. AEM. 02069-12.
69. Hartung, J.S.a.J., *Emission of Airborne Particulates from Animal Production*. Workshop 4 on Sustainable Animal Production., 2000.